



STAGGERED GRID RESIDUAL DISTRIBUTION SCHEME

Remi Abgrall, Tokareva Svetlana

► To cite this version:

Remi Abgrall, Tokareva Svetlana. STAGGERED GRID RESIDUAL DISTRIBUTION SCHEME: Staggered grid RD scheme for Lagrangian hydrodynamics. 2016. hal-01327473v2

HAL Id: hal-01327473

<https://inria.hal.science/hal-01327473v2>

Preprint submitted on 2 May 2017

HAL is a multi-disciplinary open access archive for the deposit and dissemination of scientific research documents, whether they are published or not. The documents may come from teaching and research institutions in France or abroad, or from public or private research centers.

L'archive ouverte pluridisciplinaire **HAL**, est destinée au dépôt et à la diffusion de documents scientifiques de niveau recherche, publiés ou non, émanant des établissements d'enseignement et de recherche français ou étrangers, des laboratoires publics ou privés.

STAGGERED GRID RESIDUAL DISTRIBUTION SCHEME FOR LAGRANGIAN HYDRODYNAMICS*

RÉMI ABGRALL[†] AND SVETLANA TOKAREVA[‡]

Abstract. This paper is focused on the Residual Distribution (RD) interpretation of the Dobrev et al. scheme [Dobrev et al., SISC, 2012] for the numerical solution of the Euler equations in Lagrangian form. The first ingredient of the original scheme is the staggered grid formulation which uses continuous node-based finite element approximations for the kinematic variables and cell-centered discontinuous finite elements for the thermodynamic parameters. The second ingredient of the Dobrev et al. scheme is an artificial viscosity technique applied in order to make possible the computation of strong discontinuities. The aim of this paper is to provide an efficient mass matrix diagonalization method in order to avoid the inversion of the global sparse mass matrix while keeping all the accuracy properties and to construct a parameter-free stabilization of the scheme to get rid of the artificial viscosity. In addition, we study the conservation and entropy properties of the constructed RD scheme. To demonstrate the robustness of the proposed RD scheme, we solve several one-dimensional shock tube problems from rather mild to very strong ones. This paper also illustrates a general technique that enables, from a non conservative formulation of a system that has a conservative formulation, how to design a numerical approximation that will provably give sequences of solution converging to a weak solution of the problem. This enable to use directly variables that are more pertinent, from an engineering point of view, than the standard conserved variables: here the specific internal energy.

Key words. Residual distribution scheme, Lagrangian hydrodynamics, finite elements

AMS subject classifications. 65M60, 76N15, 76L05

1. Introduction. We are interested in the numerical solution of the Euler equations in Lagrangian form. It is very well known there are two formulations of the fluid mechanics equations, depending whether the formulation is done in a fixed frame (Euler formulation) or a reference frame moving at the fluid speed (Lagrangian formulation). There is also an intermediate formulation, the ALE (for Arbitrary Eulerian Lagrangian) formulation where the reference frame is moving a speed that is generally neither zero nor the fluid velocity. Each of these formulations have advantages and drawback. The Eulerian one is conceptually the simplest because the reference frame is not moving; in term of numerics this translates by a fixed grid. The two other are conceptually more complicated because of a moving reference frame; in term of numerics this translates into a moving grid with the possibility of having a tangling mesh. However, the situation is not as simple. In computing compressible flows, one has to be able to compute two kinds of discontinuity: the shock waves and the slip lines. Slip lines are difficult to compute, most of the time not because of stability problems as for shock waves, but because of numerical dissipation. Hence dealing with a mesh that moves somewhat with the flow speed, and in this respect, the Lagrangian formulation is ideal, is a straightforward way to minimize the numerical dissipation attached to slip lines: they are steady in the Lagrangian frame. Of course the price to pay is how to handle moving meshes and the tangling problems, but this nice property of a relatively simple and efficient way to deal with slip lines has motivated many researchers, starting from the seminal work of von Neumann and Richtmyer [34], to more recent works such as [13, 25, 6, 28, 14, 15].

Most of these works deal with schemes that are formally second order accurate.

*This work was funded by SNFS via the grant # 200021_153604

[†]Institute of Mathematics, University of Zurich, Switzerland (remi.abgrall@math.uzh.ch).

[‡]Institute of Mathematics, University of Zurich, Switzerland (svetlana.tokareva@math.uzh.ch).

Up to our knowledge, there are much less works dealing with (formally) high order methods: either they are of discontinuous Galerkin type [31, 32, 33], use a staggered finite element formulation [16] or an ENO/WENO formalism [14], see also the recent developments in [8, 18, 9, 17, 7, 11, 10].

In the discontinuous Galerkin (DG) formulation, all variables are described inside elements, while in the staggered grid formulation, the approximations of the thermodynamic parameters (such as pressure, specific internal energy or volume/density) are cell-centered, and thus possibly discontinuous across elements as in the DG method, while the velocity approximation is node-based, that is, it is described by a function that is polynomial in each element and globally continuous in the whole computational domain. In a way this is a natural extension of the Wilkins' scheme [35] to higher order of accuracy.

This paper is focused on Dobrev et al. [16] formulation. This formulation, that we describe in more detail below, uses two ingredients. First, starting from the finite element formulation, one needs to introduce a global mass matrix that is block diagonal on the thermodynamic parameters (as in DG method) but leads to a sparse symmetric matrix for the velocity components (as in finite element method). Hence, the treatment of the mass matrix consists of an inversion¹ of a block diagonal matrix, which is cheap, but also of a sparse symmetric positive definite matrix, which is more expensive both in terms of CPU time and memory. In addition, every time when mesh refinement or remapping is needed (which is typical for Lagrangian methods), this global matrix needs to be recomputed. The second ingredient of the Dobrev et al. scheme is an artificial viscosity technique applied in order to make possible the computation of strong discontinuities. Note that the staggered formulation automatically guaranties linear stability.

The aim of this paper is to give answers to two questions: (i) can we avoid the inversion of the large sparse global mass matrix while keeping all the accuracy properties and (ii) can we construct a parameter-free artificial viscosity? In order to answer these questions, we rely on the Residual Distribution (RD) interpretation of the Dobrev et al. scheme and show how to modify it without introducing any additional complexity in the formulation.

The format of this contribution is as follows. We first give the formulation of the Euler equations in Lagrangian form and then recall Dobrev et al. formulation. Next, we introduce the RD formulation and show how to guarantee, when the scheme is stable, the convergence to a weak solution. Of course Dobrev et al. method satisfies these conditions, but the analysis presented in this paper opens new doors. Using the RD formulation, we show how to construct a simple first order scheme and how to increase the spatial accuracy. The next step is to explain the diagonalization of the global sparse mass matrix without the loss of accuracy: this is obtained by applying ideas coming from [27, 3]. We conclude by considering several one-dimensional shock tube problems from rather mild to very strong blast problems and a comparison between the Eulerian and lagrangian formulations.

2. Governing equations. We summarize here the derivation of the Euler equations in Lagrangian coordinates, more details can be found in [21, 29]. We consider a fluid domain $\Omega_0 \subset \mathbb{R}^d$, $d = 1, 2, 3$ that is deforming in time through the movement of the fluid, the deformed domain is denoted by Ω_t . In what follows, \mathbf{X} denotes any point of Ω_0 , while \mathbf{x} denotes any point of Ω_t , the domain obtained from Ω_0 under

¹By saying "inversion of a matrix" we mean the solution of a linear system with the corresponding matrix.

deformation. We assume the existence of a one-to-one mapping Φ from Ω_0 to Ω_t such that $\mathbf{x} = \Phi(\mathbf{X}, t) \in \Omega_t$ for any $\mathbf{X} \in \Omega_0$. We will call \mathbf{X} the Lagrangian coordinates and \mathbf{x} the Eulerian ones. The Lagrangian description corresponds to the one of an observer moving with the fluid. In particular, its velocity, which coincides with the fluid velocity, is given by:

$$(1) \quad \mathbf{u}(\mathbf{x}, t) = \frac{d\mathbf{x}}{dt} = \frac{\partial \Phi}{\partial t}(\mathbf{X}, t).$$

We also introduce the deformation tensor \mathbb{J} (Jacobian matrix),

$$(2) \quad \mathbb{J}(\mathbf{x}, t) = \nabla_{\mathbf{X}} \Phi(\mathbf{X}, t) \text{ where } \mathbf{x} = \Phi(\mathbf{X}, t).$$

Hereafter, the notation $\nabla_{\mathbf{X}}$ corresponds to the differentiation with respect to Lagrangian coordinates, while $\nabla_{\mathbf{x}}$ — to the Eulerian ones.

It is well known that the equations describing the evolution of fluid particles are consequences of the conservation of mass, momentum and energy, as well as a technical relation, the Reynolds transport theorem. It states that for any scalar quantity $\alpha(\mathbf{x}, t)$, we have:

$$(3) \quad \frac{d}{dt} \int_{\omega_t} \alpha(\mathbf{x}, t) d\mathbf{x} = \int_{\omega_t} \frac{\partial \alpha}{\partial t}(\mathbf{x}, t) d\mathbf{x} + \int_{\partial \omega_t} \alpha(\mathbf{x}, t) \mathbf{u} \cdot \mathbf{n} d\sigma = \int_{\omega_t} \left(\frac{d\alpha}{dt} + \mathbf{u} \cdot \nabla_{\mathbf{x}} \alpha \right) d\mathbf{x}$$

In this relation, the set ω_t is the image of any set $\omega_0 \subset \Omega_0$ by Φ , i.e. $\omega_t = \Phi(\omega_0, t)$, $d\sigma$ is the measure on the boundary of $\partial \omega_t$ and \mathbf{n} is the outward unit normal. The gradient operator is taken with respect to the Eulerian coordinates.

The conservation of mass reads: for any $\omega_0 \subset \Omega_0$,

$$(4) \quad \frac{d}{dt} \int_{\omega_t} \rho d\mathbf{x} = 0, \quad \omega_t = \Phi(\omega_0, t),$$

so that we get, defining $J(\mathbf{x}, t) = \det \mathbb{J}(\mathbf{x}, t)$,

$$(5) \quad J(\mathbf{x}, t) \rho(\mathbf{x}, t) = \rho(\mathbf{X}, 0) := \rho_0(\mathbf{X}).$$

Using Reynolds' transport theorem (3), we get that for any function f (real or vectorial),

$$(6) \quad \frac{d}{dt} \int_{\omega_t} \rho f d\mathbf{x} = \int_{\omega_t} \rho \frac{df}{dt} d\mathbf{x}.$$

Newton's law states that the acceleration is equal to the sum of external forces, so that

$$(7) \quad \frac{d}{dt} \int_{\omega_t} \rho \mathbf{u} d\mathbf{x} = - \int_{\partial \omega_t} p \mathbf{n} d\sigma,$$

and thus, using (3),

$$(8) \quad \rho \frac{d\mathbf{u}}{dt} + \nabla_{\mathbf{x}} p = 0.$$

The pressure $p(\mathbf{x}, t)$ is a thermodynamic characteristic of a fluid and in the simplest case a function of two independent thermodynamic parameters, for example the specific energy ε and the density,

$$(9) \quad p = p(\rho, \varepsilon).$$

The total energy of a fluid particle is $\rho e = \rho \varepsilon + \frac{1}{2} \rho \mathbf{u}^2$. Using the first principle of thermodynamics, the variation of energy is the sum of variations of heat and the work of the external forces. Assuming an isolated system, we get

$$\frac{d}{dt} \int_{\omega_t} \rho \left(\varepsilon + \frac{1}{2} \mathbf{u}^2 \right) d\mathbf{x} = - \int_{\partial \omega_t} p \mathbf{u} \cdot \mathbf{n} d\sigma,$$

i.e.

$$(8) \quad \rho \frac{d\varepsilon}{dt} + p \nabla_{\mathbf{x}} \cdot \mathbf{u} = 0.$$

In this paper, we are interested in solving the set of equations (1)(2), (4) and (8) with the EOS of the form (7):

$$\begin{aligned} \mathbf{u}(\mathbf{x}, t) &= \frac{d\mathbf{x}}{dt}, \mathbf{x} = \Phi(\mathbf{X}, t) \\ J(\mathbf{x}, t) \rho(\mathbf{x}, t) &= \rho(\mathbf{X}, 0) := \rho_0(\mathbf{X}), \\ \rho \frac{d\mathbf{u}}{dt} + \nabla_{\mathbf{x}} p &= 0 \\ \rho \frac{d\varepsilon}{dt} + p \nabla_{\mathbf{x}} \cdot \mathbf{u} &= 0. \end{aligned}$$

where

$$(9b) \quad p = p(\rho, \varepsilon).$$

In addition, we have the constraint that the physical specific entropy s is increasing across shock waves

$$\frac{ds}{dt} \geq 0.$$

Introducing the specific volume $v = \frac{1}{\rho}$, from the Gibbs relation $T ds = d\varepsilon + p dv$, this amounts to

$$\frac{d\varepsilon}{dt} + p \frac{dv}{dt} \geq 0.$$

3. Staggered grid scheme of Dobrev et al. Here we briefly recall the main ideas of the staggered grid method proposed in [16]. The semi-discrete approximation of (9) is sought for such that the velocity field \mathbf{u} belongs to a kinematic space $\mathcal{V} \subset (H^1(\Omega_0))^d$ of finite dimension; it has a basis denoted by $\{w_{i_{\mathcal{V}}}\}_{i_{\mathcal{V}} \in \mathcal{D}_{\mathcal{V}}}$, the set $\mathcal{D}_{\mathcal{V}}$ is the set of kinematic degrees of freedom (DOFs) with the total number of DOFs given by $\#\mathcal{D}_{\mathcal{V}} = N_{\mathcal{V}}$. The thermodynamic quantities such as the internal energy ε are sought for in a thermodynamic space $\mathcal{E} \subset L^2(\Omega_0)$. As before, this space is finite dimensional, and its basis is $\{\phi_{i_{\mathcal{E}}}\}_{i_{\mathcal{E}} \in \mathcal{D}_{\mathcal{E}}}$. The set $\mathcal{D}_{\mathcal{E}}$ is the set of thermodynamical degrees of freedom with the total number of DOFs $\#\mathcal{D}_{\mathcal{E}} = N_{\mathcal{E}}$. In the following, the subscript \mathcal{V} (resp. \mathcal{E}) refers to kinematic (resp. thermodynamic) degrees of freedom.

The fluid particle position \mathbf{x} is approximated by:

$$(10a) \quad \mathbf{x} = \Phi(\mathbf{X}, t) = \sum_{i_{\mathcal{V}} \in \mathcal{D}_{\mathcal{V}}} \mathbf{x}_{i_{\mathcal{V}}}(t) w_{i_{\mathcal{V}}}(\mathbf{X}).$$

The domain at time t is then defined by

$$\Omega(t) = \{\mathbf{x} \in \mathbb{R}^d \text{ such that } \exists \mathbf{X} \in \Omega_0 : \mathbf{x} = \Phi(\mathbf{X}, t)\}$$

where Φ is given by (10a).

The velocity field is approximated by:

$$(10b) \quad \mathbf{u}(\mathbf{x}, t) = \sum_{i_{\mathcal{V}} \in \mathcal{D}_{\mathcal{V}}} \mathbf{u}_{i_{\mathcal{V}}}(t) w_{i_{\mathcal{V}}}(\mathbf{X}),$$

and the specific internal energy is given by:

$$(10c) \quad \varepsilon(\mathbf{x}, t) = \sum_{i_{\mathcal{E}} \in \mathcal{D}_{\mathcal{E}}} \varepsilon_{i_{\mathcal{E}}}(t) \phi_{i_{\mathcal{E}}}(\mathbf{X}).$$

Considering the weak formulation of (9), we get:

1. For the velocity equation, for any $i_{\mathcal{V}} \in \mathcal{D}_{\mathcal{V}}$, denoting by \mathbf{n} the outward pointing unit vector of $\partial\Omega(t)$,

$$(10d) \quad \int_{\Omega_t} \rho \frac{d\mathbf{u}}{dt} w_{i_{\mathcal{V}}} d\mathbf{x} = - \int_{\Omega_t} \boldsymbol{\tau} : \nabla_{\mathbf{x}} w_{i_{\mathcal{V}}} d\mathbf{x} + \int_{\partial\Omega_t} \mathbf{n} \cdot \boldsymbol{\tau} \cdot w_{i_{\mathcal{V}}} d\sigma$$

where for now, the stress tensor $\boldsymbol{\tau}$ is defined as $\boldsymbol{\tau} = -p\mathbf{Id}$.²

Using (10b), we get³

$$\sum_{j_{\mathcal{V}}} \left(\int_{\Omega_t} \rho w_{j_{\mathcal{V}}} w_{i_{\mathcal{V}}} d\mathbf{x} \right) \frac{d\mathbf{u}_{j_{\mathcal{V}}}}{dt} = - \int_{\Omega_t} \boldsymbol{\tau} : \nabla_{\mathbf{x}} w_{i_{\mathcal{V}}} d\mathbf{x} + \int_{\partial\Omega_t} \mathbf{n} \cdot \boldsymbol{\tau} \cdot w_{i_{\mathcal{V}}} d\sigma.$$

Introducing the vector $\hat{\mathbf{u}}$ with components $\mathbf{u}_{i_{\mathcal{V}}}$ and \mathbf{F} the force vector given by the right-hand side of the above equation, we get the formulation

$$\mathbf{M}_{\mathcal{V}} \frac{d\hat{\mathbf{u}}}{dt} = \mathbf{F}.$$

The kinematic mass matrix $\mathbf{M}_{\mathcal{V}} = (M_{i_{\mathcal{V}}j_{\mathcal{V}}})$ has components

$$M_{i_{\mathcal{V}}j_{\mathcal{V}}} = \int_{\Omega_t} \rho w_{j_{\mathcal{V}}} w_{i_{\mathcal{V}}} d\mathbf{x}.$$

Thanks to the Reynolds transport theorem (3) and mass conservation, $\mathbf{M}_{\mathcal{V}}$ does not depend on time, see [16] for details.

2. For the internal energy, we get a similar form,

$$(10e) \quad \int_{\Omega_t} \rho \frac{d\varepsilon}{dt} \phi_{i_{\mathcal{E}}} d\mathbf{x} = \int_{\Omega_t} \phi_{i_{\mathcal{E}}} \boldsymbol{\tau} : \nabla_{\mathbf{x}} \mathbf{u} d\mathbf{x},$$

which leads to

$$\mathbf{M}_{\mathcal{E}} \frac{d\hat{\varepsilon}}{dt} = \mathbf{W},$$

where $\hat{\varepsilon}$ is the vector with components $\varepsilon_{i_{\mathcal{E}}}$, the thermodynamic mass matrix $\mathbf{M}_{\mathcal{E}} = (M_{i_{\mathcal{E}}j_{\mathcal{E}}})$ with entries $M_{i_{\mathcal{E}}j_{\mathcal{E}}} = \int_{\Omega_t} \phi_{i_{\mathcal{E}}} \phi_{j_{\mathcal{E}}} d\mathbf{x}$ is again independent of time and \mathbf{W} is the right-hand side of (10e).

3. The mass satisfies:

$$(10f) \quad \det \mathbb{J}(\mathbf{x}, t) \rho(\mathbf{x}, t) = \rho_0(\mathbf{X})$$

where $\rho_0 \in \mathcal{E}$. The deformation tensor \mathbb{J} is evaluated according to (10a).

²Here, if \mathbf{X} is a tensor and \mathbf{y} is a vector, $\mathbf{X} \cdot \mathbf{y}$ is the usual matrix-vector multiplication.

³Here, if \mathbf{X} and \mathbf{Y} are tensors, $\mathbf{X} : \mathbf{Y}$ is the contraction $\mathbf{X} : \mathbf{Y} = \text{trace}(\mathbf{X}^T \mathbf{Y})$.

4. The positions \mathbf{x}_{i_V} satisfy:

$$(10g) \quad \frac{d\mathbf{x}_{i_V}}{dt} = \mathbf{u}_{i_V}(\mathbf{x}_{i_V}, t)$$

It remains to define the spaces \mathcal{V} and \mathcal{E} . To do this, we consider a *conformal* triangulation of the initial computational domain $\Omega_0 \subset \mathbb{R}^d$, $d = 1, 2, 3$, which we shall denote by \mathcal{T}_h . We denote by K any element of \mathcal{T}_h and assume for simplicity that $\cup_K K = \Omega_0$. The set of boundary faces is denoted by \mathcal{B} and a generic boundary face is denoted by f , thus $\cup_{f \in \mathcal{B}} f = \partial\Omega_0$. As usual, denoting by $\mathbb{P}^r(K)$ the set of polynomials of degree r defined on K , we consider two functional spaces (with integer $r \geq 1$):

$$\mathcal{V} = \{\mathbf{v} \in L^2(\Omega_0)^d, \forall K, \mathbf{v}|_K \in \mathbb{P}^r(K)^d\} \cap C^0(\Omega_0)$$

and

$$\mathcal{E} = \{\theta \in L^2(\Omega_0), \forall K, \theta|_K \in \mathbb{P}^{r-1}(K)\}.$$

Clearly, for any t , $x \in \Omega_t$, the Jacobian J is a priori not continuous across the faces of elements, and hence the relation (10f) is to be understood in the interior of elements. The matrix $\mathbf{M}_{\mathcal{E}}$ is symmetric positive definite block-diagonal while $\mathbf{M}_{\mathcal{V}}$ is only a *sparse* symmetric positive definite matrix.

The fundamental assumption made here is that the mapping Φ is bijective. In numerical situations, this can be hard to achieve for long term simulations, and thus mesh remapping and re-computation of the matrices $\mathbf{M}_{\mathcal{E}}$ and $\mathbf{M}_{\mathcal{V}}$ must be done from time to time; this issue is however outside of the scope of this paper, see [29] for detailed discussion.

The scheme defined by (10) is only linearly stable. Since we are looking for possibly discontinuous solutions, in the original scheme of Dobrev et al. a mechanism of artificial viscosity is added. The idea amounts to modifying the stress tensor $\boldsymbol{\tau} = -p\mathbf{Id}_d$ by $\boldsymbol{\tau} = -p\mathbf{Id}_d + \boldsymbol{\tau}_a(\mathbf{x}, t)$, where the term $\boldsymbol{\tau}_a(\mathbf{x}, t)$ specifies the artificial viscosity. We refer to [16] for details on the construction of $\boldsymbol{\tau}_a(\mathbf{x}, t)$.

It is possible to rewrite the system (9), and in particular the relations (10d) and (10e) in a slightly different way. Let K be any element of the triangulation \mathcal{T}_h , and for the kinematic degrees of freedom $i_V \in \mathcal{D}_V$ and the thermodynamic degrees of freedom $i_{\mathcal{E}} \in \mathcal{D}_{\mathcal{E}}$ consider the quantities

$$\begin{aligned} \Phi_{V, i_V}^K &= \int_K \boldsymbol{\tau} : \nabla_{\mathbf{x}} w_{i_V} d\mathbf{x} - \int_{\partial K} \hat{\boldsymbol{\tau}}_{\mathbf{n}} w_{i_V} d\sigma, \\ \Phi_{\mathcal{E}, i_{\mathcal{E}}}^K &= - \int_K \phi_{i_{\mathcal{E}}}^K \boldsymbol{\tau} : \nabla_{\mathbf{x}} \mathbf{u} d\mathbf{x}, \end{aligned}$$

where $\hat{\boldsymbol{\tau}}_{\mathbf{n}}$ is any numerical flux consistent with $\boldsymbol{\tau} \cdot \mathbf{n}$, see e. g. [30].

Using the compactness of the support of the basis functions w_{i_V} and $\phi_{i_{\mathcal{E}}}$, we can rewrite the relations (10d) and (10e) as follows⁴:

$$(11a) \quad \int_{\Omega_t} \rho \frac{d\mathbf{u}}{dt} w_{i_V} d\mathbf{x} + \sum_{K \ni i_V} \Phi_{V, i_V}^K = 0$$

⁴In what follows, given a quantity $\{a_{i_V}^K\}$ defined for each element K and each velocity degree of freedom contained in that element (hence, for one velocity degree of freedom, we can have several values, depending from which element we are looking at i_V), and given any velocity degree of freedom i_V , the sum $\sum_{K \ni i_V} a_{i_V}^K$ represents the sum of all the terms $a_{i_V}^K$ for all the element that share this degree of freedom. A similar notation is used for the thermodynamic degree of freedom. See figure 1 for a graphical illustration.

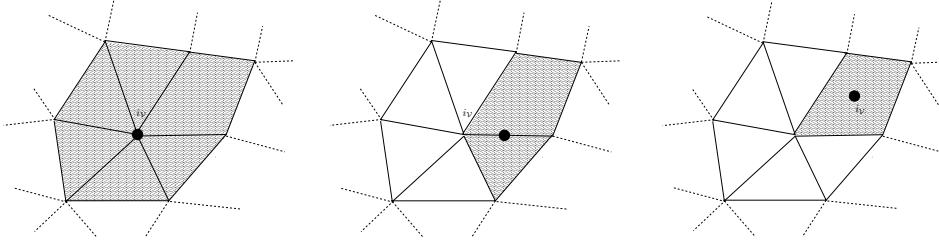


FIG. 1. The shaded area represent the union of the neighboring elements containing the degree of freedom i_V in diverse configurations.

and

$$(11b) \quad \int_{\Omega_t} \rho \frac{d\varepsilon}{dt} \phi_{i_\varepsilon} d\mathbf{x} + \sum_{K \ni i_\varepsilon} \Phi_{\mathcal{E}, i_\varepsilon}^K = 0,$$

and we notice that on each element K , we have:

$$(11c) \quad \sum_{i_\varepsilon \in K} \Phi_{\mathcal{E}, i_\varepsilon}^K + \sum_{i_V \in K} \mathbf{u}_{i_V} \cdot \Phi_{\mathcal{V}, i_V}^K \\ = - \sum_{i_\varepsilon \in K} \int_K \phi_{i_\varepsilon}^K \boldsymbol{\tau} : \nabla_{\mathbf{x}} \mathbf{u} d\mathbf{x} + \sum_{i_V \in K} \left(\mathbf{u}_{i_V} \cdot \int_K \boldsymbol{\tau} : \nabla_{\mathbf{x}} w_{i_V} d\mathbf{x} - \mathbf{u}_{i_V} \cdot \int_{\partial K} \hat{\boldsymbol{\tau}}_{\mathbf{n}} w_{i_V} d\sigma \right) \\ = - \int_K \boldsymbol{\tau} : \nabla_{\mathbf{x}} \mathbf{u} d\mathbf{x} + \int_K \boldsymbol{\tau} : \nabla_{\mathbf{x}} \mathbf{u} d\mathbf{x} - \int_{\partial K} \hat{\boldsymbol{\tau}}_{\mathbf{n}} \cdot \mathbf{u} d\sigma = - \int_{\partial K} \hat{\boldsymbol{\tau}}_{\mathbf{n}} \cdot \mathbf{u} d\sigma.$$

There is no ambiguity in the definition of the last integral in (11c) because \mathbf{u} is continuous across ∂K and the numerical flux $\hat{\boldsymbol{\tau}}_{\mathbf{n}}$ is well defined.

Since we have the relation (11c) and a similar relation for the total momentum, namely

$$(12) \quad \sum_{i_V \in K} \Phi_{\mathcal{V}, i_V}^K = - \int_{\partial K} \boldsymbol{\tau} \cdot \mathbf{n} d\sigma,$$

and since the flux $\hat{\boldsymbol{\tau}}_{\mathbf{n}}$ is consistent with $\boldsymbol{\tau} \cdot \mathbf{n}$, one can easily show using the same argument as in [5] that:

1. if we use a sequence of meshes which typical mesh size tends to 0, while staying shape regular in the sense of classical finite element,
 2. if the numerical solution stay component-wise bounded in L^∞ , converges (component-wise) in L^2 towards some function (\mathbf{u}, e)
- then this solution is a weak solution of the initial problem.

In addition, we have a positive balance of entropy as soon as $\boldsymbol{\tau}_a : \nabla u \geq 0$ in each element since

$$\int_K \rho T \frac{ds}{dt} d\mathbf{x} = \int_K \rho \left(\frac{d\varepsilon}{dt} + p \frac{d(1/\rho)}{dt} \right) d\mathbf{x} \\ = \int_K \left(\rho \frac{d\varepsilon}{dt} + p \nabla_{\mathbf{x}} \mathbf{u} \right) d\mathbf{x} = \int_K (\boldsymbol{\tau}_a : \nabla_{\mathbf{x}} \mathbf{u}) d\mathbf{x} \geq 0.$$

4. Residual distribution formulation. In this section, we briefly recall the concept of residual distribution schemes for the following problem in $\Omega \subset \mathbb{R}^d$:

$$\frac{\partial u}{\partial t} + \nabla_{\mathbf{x}} \cdot \mathbf{f}(u) = 0$$

with the initial condition $u(\mathbf{x}, 0) = u_0(\mathbf{x})$. For simplicity we assume that u is a real-valued function. Again, we consider a triangulation \mathcal{T}_h of Ω . We want to approximate u in

$$V_h = \{u \in L^2(\Omega), \text{ for any } K \in \mathcal{T}_h, u|_K \in \mathbb{P}^r\} \cap C^0(\Omega).$$

The set $\{\varphi_i\}$ is a basis of V_h , and u_i are such that $u = \sum_i u_i \varphi_i$. As usual, h represents the maximal diameter of the element of \mathcal{T}_h . We use the same notations as before, and here the index i denotes a generic degree of freedom.

We start by the steady version of this problem,

$$\nabla_{\mathbf{x}} \cdot \mathbf{f}(u) = 0$$

and omit, for the sake of simplicity, the boundary conditions, see [1] for details. We consider schemes of the form:

$$(13) \quad \sum_{K \ni i} \Phi_i^K(u) = 0 \quad \forall i,$$

with

$$\Phi_i^K(u) = \int_K \varphi_i \nabla_{\mathbf{x}} \cdot \mathbf{f}(u) d\mathbf{x}.$$

The residuals must satisfy the conservation relation: for any K ,

$$(14) \quad \sum_{i \in K} \Phi_i^K(u) = \int_{\partial K} \mathbf{f}^h \cdot \mathbf{n} d\sigma := \Phi^K(u).$$

Here, $\mathbf{f}^h \cdot \mathbf{n}$ is an $(r+1)$ -th order approximation of $\mathbf{f}(u) \cdot \mathbf{n}$. Given a sequence of meshes that are shape regular with $h \rightarrow 0$, one can construct a sequence of solution. In [5], it is shown that, if (i) this sequence of solutions stays bounded in L^∞ , (ii) a sub-sequence of it converges in $L^2(\Omega)$ towards a limit u and (iii) the residuals are continuous with respect to u , then the conservation condition guaranties that u is a weak solution of the problem.

A typical example of such residual is the Rusanov residual,

$$\Phi_i^{K, \text{Rus}}(u) = - \int_K \nabla_{\mathbf{x}} \varphi_i \cdot \mathbf{f}^h d\mathbf{x} + \int_{\partial K} \mathbf{f}^h \cdot \mathbf{n} \varphi_i d\sigma + \alpha_K (u_i - \bar{u}_K),$$

where

$$\bar{u}_K = \frac{1}{N_K} \sum_{j \in K} u_j$$

with N_K being the number of degrees of freedom inside an element K and

$$\alpha_K \geq \max_{\mathbf{x} \in K, \mathbf{n}, \|\mathbf{n}\|=1} \rho(\nabla_{\mathbf{u}} \mathbf{f}(u) \cdot \mathbf{n}).$$

Here, $\rho(A)$ is the spectral radius of the matrix A .

This residual can be rewritten as

$$\Phi_i^{K,\text{Rus}}(u) = \sum_{j \in K} c_{ij}^K (u_i - u_j)$$

with $c_{ji}^K \geq 0$. It is easy to see that using the Rusanov residual leads to very dissipative solutions, but the scheme is easily shown to be monotonicity preserving in the scalar case, see for example [5]. In the system case, one can see that . There is a systematic way of improving the accuracy. One can show [5] that if the residuals satisfy, for any degree of freedom i ,

$$\Phi_i^K(u_{ex}^h) = O(h^{k+d}),$$

where u_{ex} is the exact solution of the steady problem, u_{ex}^h is an interpolation of order $k+1$ and d is the dimension of the problem, then the scheme is formally of order $k+1$. It is shown in [5] how to achieve a high order of accuracy while keeping the monotonicity preserving property. A systematic way of achieving this is to set:

$$(15) \quad \Phi_i^K(u) = \beta_i^K(u) \Phi^K(u),$$

where

$$(16) \quad \beta_i^K(u) = \frac{\max\left(\frac{\Phi_i^{K,\text{Rus}}}{\Phi^K}, 0\right)}{\sum_{j \in K} \max\left(\frac{\Phi_j^{K,\text{Rus}}}{\Phi^K}, 0\right)}$$

and Φ^K is defined by (14). Some refinements exist in order to get an entropy inequality, see [4, 1] for example. Note that $\beta_i^K(u)$ is constant on K .

It is easy to see that one can rewrite (15) in a Petrov-Galerkin fashion:

$$\begin{aligned} \Phi_i^K(u) &= \int_K \beta_i^K(u) \nabla_{\mathbf{x}} \cdot \mathbf{f}^h d\mathbf{x} = \int_K \varphi_i \nabla_{\mathbf{x}} \cdot \mathbf{f}^h d\mathbf{x} + \int_K (\beta_i^K(u) - \varphi_i) \nabla_u f \cdot \nabla_{\mathbf{x}} u d\mathbf{x} \\ &= - \int_K \nabla_{\mathbf{x}} \varphi_i \cdot \mathbf{f} d\mathbf{x} + \int_{\partial K} \varphi_i \mathbf{f} \cdot \mathbf{n} d\sigma + \int_K (\beta_i^K(u) - \varphi_i) \nabla_u \mathbf{f} \cdot \nabla_{\mathbf{x}} u d\mathbf{x}, \end{aligned}$$

so that from (13) we get

$$0 = - \int_{\Omega} \nabla_{\mathbf{x}} \varphi_i \cdot \mathbf{f} d\mathbf{x} + \int_{\partial \Omega} \varphi_i \mathbf{f}(u) \cdot \mathbf{n} d\sigma + \sum_{K \ni i} \int_K (\beta_i^K(u) - \varphi_i) \nabla_u \mathbf{f} \cdot \nabla_{\mathbf{x}} u d\mathbf{x}.$$

Inspired by this formulation, we would naturally discretize the unsteady problem as:

$$\begin{aligned} (17) \quad 0 &= \int_{\Omega} \varphi_i \frac{\partial u}{\partial t} d\mathbf{x} - \int_{\Omega} \nabla_{\mathbf{x}} \varphi_i \cdot \mathbf{f} d\mathbf{x} + \int_{\partial \Omega} \varphi_i \mathbf{f}(u) \cdot \mathbf{n} d\sigma \\ &\quad + \sum_{i \ni K} \int_K (\beta_i^K(u) - \varphi_i) \left(\frac{\partial u}{\partial t} + \nabla_u \mathbf{f} \cdot \nabla_{\mathbf{x}} u \right) d\mathbf{x}. \end{aligned}$$

The formulation (17) can be as well derived from (13) by introducing the "space-time" residuals (the value of β_i^K is not relevant at this stage)

$$(18) \quad \Phi_i^K(u) = \beta_i^K(u) \int_K \left(\frac{\partial u}{\partial t} + \nabla_{\mathbf{x}} \cdot \mathbf{f}(u) \right) d\mathbf{x}.$$

The semi-discrete scheme (17) requires an appropriate ODE solver for time-stepping.

A straightforward discretization of (17) would lead to a mass matrix $\mathbf{M} = (M_{ij})_{i,j}$ with entries

$$M_{ij} = \int_{\Omega} \varphi_i \varphi_j d\mathbf{x} + \sum_{i \ni K} \int_K (\beta_i^K(u) - \varphi_i) \varphi_j d\mathbf{x}.$$

Unfortunately, this matrix has no special structure, might not be invertible (so the problem is not even well posed!), and in any case it is highly non linear since β_i^K depends on u . A solution to circumvent the problem has been proposed in [27]. The main idea is to keep the spatial structure of the scheme and slightly modify the temporal one without violating the formal accuracy. A second order version of the method is designed in [27] and extension to high order is explained in [3]. For the purposes of this paper and for comparison with [16] we only need the second order case.

Here we describe the idea of the modified time stepping from [27]. We start with the description of our time-stepping algorithm based on a second order Runge-Kutta scheme for an ODE of the form

$$y' + L(y) = 0.$$

Given an approximate solution y_n at time t^n , for the calculation of y_{n+1} we proceed as follows:

1. set $y^{(0)} = y^n$;
2. compute $y^{(1)}$ defined by

$$\frac{y^{(1)} - y^{(0)}}{\Delta t} + L(y^{(0)}) = 0;$$

3. compute $y^{(2)}$ defined by

$$\frac{y^{(2)} - y^{(0)}}{\Delta t} + \frac{L(y^{(0)}) + L(y^{(1)})}{2} = 0;$$

4. set $y^{n+1} = y^{(2)}$.

We see that the generic step in this scheme has the form

$$\frac{\delta^k y}{\Delta t} + \mathcal{L}(y^{(0)}, y^{(k)}) = 0$$

with

$$\mathcal{L}(a, b) = \frac{L(a) + L(b)}{2}$$

and

$$\delta^k y = y^{(k+1)} - y^{(0)}, \quad k = 0, 1.$$

Coming back to the residuals (18), we write for each element K and $k = 0, 1$:

$$\begin{aligned} & \beta_i^K(u) \int_K \left(\frac{\delta^k u}{\Delta t} + \mathcal{L}(u^{(0)}, u^{(k)}) \right) d\mathbf{x} \\ &= \int_K \varphi_i \left(\frac{\delta^k u}{\Delta t} + \mathcal{L}(u^{(0)}, u^{(k)}) \right) d\mathbf{x} + \int_K (\beta_i^K(u) - \varphi_i) \left(\frac{\delta^k u}{\Delta t} + \mathcal{L}(u^{(0)}, u^{(k)}) \right) d\mathbf{x} \\ &\approx \int_K \varphi_i \left(\frac{\delta^k u}{\Delta t} + \mathcal{L}(u^{(0)}, u^{(k)}) \right) d\mathbf{x} + \int_K (\beta_i^K(u) - \varphi_i) \left(\widetilde{\frac{\delta^k u}{\Delta t}} + \mathcal{L}(u^{(0)}, u^{(k)}) \right) d\mathbf{x} \end{aligned}$$

345 with

$$346 \quad \widetilde{\delta^k y} = \begin{cases} 0 & \text{if } k = 0, \\ u^{(1)} - u^{(0)} & \text{if } k = 1. \end{cases}$$

347 We see that

$$348 \quad \int_K \varphi_i \left(\frac{\delta^k u}{\Delta t} + \mathcal{L}(u^{(0)}, u^{(k)}) \right) d\mathbf{x} + \int_K (\beta_i^K(u) - \varphi_i) \left(\frac{\widetilde{\delta^k u}}{\Delta t} + \mathcal{L}(u^{(0)}, u^{(k)}) \right) d\mathbf{x} \\ 349 \quad = \int_K \varphi_i \left(\frac{\delta^k u}{\Delta t} - \frac{\widetilde{\delta^k u}}{\Delta t} \right) d\mathbf{x} + \beta_i^K(u) \int_K \left(\frac{\widetilde{\delta^k u}}{\Delta t} + \mathcal{L}(u^{(0)}, u^{(k)}) \right) d\mathbf{x}. \\ 350 \\ 351$$

352 This relation is further simplified if mass lumping can be applied: letting

$$353 \quad (19) \quad C_i^K = \sum_{j \in K} \int_K \varphi_i \varphi_j d\mathbf{x} = \int_K \varphi_i d\mathbf{x}$$

354 and

$$355 \quad (20) \quad C_i = \int_{\Omega} \varphi_i d\mathbf{x} = \sum_{K \ni i} \int_K \varphi_i d\mathbf{x},$$

356 for the degree of freedom i and the element K we look at the quantity

$$357 \quad C_i^K \left(\frac{\delta^k u_i}{\Delta t} - \frac{\widetilde{\delta^k u_i}}{\Delta t} \right) + \beta_i^K(u) \int_K \left(\frac{\widetilde{\delta^k u}}{\Delta t} + \mathcal{L}(u^{(0)}, u^{(k)}) \right) d\mathbf{x},$$

358 i.e.

$$359 \quad C_i^K \frac{u_i^{(k+1)} - u_i^{(k)}}{\Delta t} + \beta_i^K(u) \int_K \left(\frac{\widetilde{\delta^k u}}{\Delta t} + \mathcal{L}(u^{(0)}, u^{(k)}) \right) d\mathbf{x}.$$

360 Here $\beta_i^K(u)$ is evaluated using (16) where $\Phi_i^{K, \text{Rus}}$ is replaced by the modified space-
361 time Rusanov residuals

$$362 \quad \Phi_i^{K, \text{Rus}} = \int_K \varphi_i \left(\frac{\widetilde{\delta^k u}}{\Delta t} + \mathcal{L}(u^{(0)}, u^{(k)}) \right) d\mathbf{x} + \frac{1}{2} \left(\alpha_K^{(0)} (u_i^{(0)} - \bar{u}_K^{(0)}) + \alpha_K^{(k)} (u_i^{(k)} - \bar{u}_K^{(k)}) \right),$$

363 where

$$364 \quad \bar{u}^{(l)} = \frac{1}{N_K} \sum_{j \in K} u_j^{(l)}, \quad l = 0, k,$$

365 with N_K being the number of degrees of freedom in an element K and α_K large
366 enough and, finally,

$$367 \quad \Phi^K(u) = \sum_{i \in K} \Phi_i^{K, \text{Rus}}.$$

368 Then the idea is to use (13) at each step of the Runge-Kutta method with the residuals
369 given by

$$370 \quad (21) \quad \Phi_i^K(u) = \int_K \varphi_i \left(\frac{\delta^k u}{\Delta t} + \mathcal{L}(u^{(0)}, u^{(k)}) \right) d\mathbf{x} \\ 371 \quad + \int_K (\beta_i^K(u) - \varphi_i) \left(\frac{\widetilde{\delta^k u}}{\Delta t} + \mathcal{L}(u^{(0)}, u^{(k)}) \right) d\mathbf{x}, \\ 372 \\ 373$$

so that the overall step writes: for $k = 0, 1$ and any i ,

$$(22) \quad C_i \frac{u_i^{(k+1)} - u_i^{(k)}}{\Delta t} + \sum_{K \ni i} \Phi_{i,ts}^{K,L} = 0,$$

where we have introduced the limited space-time residuals

$$(23) \quad \Phi_{i,ts}^{K,L} = \beta_i^K \int_K \left(\frac{\delta^k u}{\Delta t} + \mathcal{L}(u^{(0)}, u^{(k)}) \right) d\mathbf{x}.$$

One can easily see that each step of (22) is purely explicit.

One can show that this scheme is second order in time. The *key* reason for this is that we have

$$\sum_{i \in K} \int_K (\varphi_i - \beta_i^K(u)) d\mathbf{x} = 0,$$

see [27, 4, 1] for details.

REMARK 4.1. *We need that $C_i > 0$ for any degree of freedom. This might not hold, for example, for quadratic Lagrange basis. For this reason, we will use Bézier elements for the approximation of the solution.*

5. Residual distribution scheme for Lagrangian hydrodynamics. In this section, we explain how to adapt the previous framework to the equations of Lagrangian hydrodynamics. We consider the same functional spaces as in section 3, namely the kinematic space \mathcal{V} and the thermodynamic space \mathcal{E} .

In the case of a simplex $K \subset \mathbb{R}^d$, one can consider the barycentric coordinates associated to the vertices of K and denoted by $\{\Lambda_j\}_{j=1,d+1}$. By definition, the barycentric coordinates are positive on K and we can consider the Bézier polynomials of degree r : define $r = i_1 + \dots + i_{d+1}$, then

$$(24) \quad B_{i_1 \dots i_{d+1}} = \frac{r!}{i_1! \dots i_{d+1}!} \Lambda_1^{i_1} \dots \Lambda_{d+1}^{i_{d+1}}.$$

Clearly, $B_{i_1 \dots i_{d+1}} \geq 0$ on K and using the binomial identity

$$\sum_{i_1, \dots, i_{d+1}, \sum_1^{d+1} i_j = r} B_{i_1 \dots i_{d+1}} = \left(\sum_{i=1}^{d+1} \Lambda_i \right)^r = 1.$$

It is left to define the residuals for the equations of the Lagrangian hydrodynamics. Since the PDE on the velocity is written in conservation form, this is only a mild adaptation of the derivations presented in the previous section, at least in the 1D case when the velocity is a scalar. In the multidimensional case, one can follow [27]. However, we need to introduce some modifications for the thermodynamics. To this end, we first focus on the spatial term, in the spirit of [27, 4]. We construct a first order monotone scheme, and using the technique of [4], we design a formally high order accurate scheme. Therefore, we introduce the total residuals

$$(25) \quad \Phi^K = \int_{\partial K} \hat{p}_n d\sigma \quad \text{and} \quad \Psi^K = \int_K p \nabla_{\mathbf{x}} \cdot \mathbf{u} d\mathbf{x},$$

where $p \in \mathcal{E}$, $u \in \mathcal{V}$ and \hat{p}_n is a consistent numerical flux which depends on the left and right state at ∂K . Next, the Galerkin residuals are given by

$$\begin{aligned} \Phi_{i_{\mathcal{V}}}^K &= - \int_K p \nabla_{\mathbf{x}} \phi_{i_{\mathcal{V}}} d\mathbf{x} + \int_{\partial K} \phi_{i_{\mathcal{V}}} \hat{p}_n d\sigma, \\ \Psi_{i_{\mathcal{E}}}^K &= \int_K \psi_{i_{\mathcal{E}}} p \nabla_{\mathbf{x}} \cdot \mathbf{u} d\mathbf{x}. \end{aligned} \quad (26)$$

From (26), we define the Rusanov residuals

$$\Phi_{i_{\mathcal{V}}}^{K,\text{Rus}}(\mathbf{u}, \varepsilon) = \Phi_{i_{\mathcal{V}}}^K(\mathbf{u}, \varepsilon) + \alpha_K(\mathbf{u}_{i_{\mathcal{V}}} - \bar{\mathbf{u}}), \quad \bar{\mathbf{u}} = \frac{1}{N_{\mathcal{V}}^K} \sum_{i_{\mathcal{V}} \in K} \mathbf{u}_{i_{\mathcal{V}}} \quad (27)$$

and

$$\Psi_{i_{\mathcal{E}}}^{K,\text{Rus}}(\mathbf{u}, \varepsilon) = \Psi_{i_{\mathcal{E}}}^K(\mathbf{u}, \varepsilon) + \alpha_K(\varepsilon_{i_{\mathcal{E}}} - \bar{\varepsilon}), \quad \bar{\varepsilon} = \frac{1}{N_{\mathcal{E}}^K} \sum_{i_{\mathcal{E}} \in K} \varepsilon_{i_{\mathcal{E}}} \quad (28)$$

where α_K is an upper bound of the Lagrangian speed of sound ρc on K and $N_{\mathcal{V}}^K$ (resp. $N_{\mathcal{E}}^K$) is the number of degrees of freedom for the velocity (resp. energy) on K .

The temporal discretization is done using the technique developed in the previous section. We introduce the modified space-time Rusanov residuals, for $k = 0, 1$:

$$\Phi_{i_{\mathcal{V}},ts}^{K,\text{Rus}} = \int_K \varphi_{i_{\mathcal{V}}} \rho \frac{\widetilde{\delta^k \mathbf{u}}}{\Delta t} d\mathbf{x} + \frac{1}{2} \left(\Phi_{i_{\mathcal{V}}}^{K,\text{Rus}}(\mathbf{u}^{(0)}, \varepsilon^{(0)}) + \Phi_{i_{\mathcal{V}}}^{K,\text{Rus}}(\mathbf{u}^{(k)}, \varepsilon^{(k)}) \right) \quad (29)$$

and

$$\Psi_{i_{\mathcal{E}},ts}^{K,\text{Rus}} = \int_K \psi_{i_{\mathcal{E}}} \rho \frac{\widetilde{\delta^k \varepsilon}}{\Delta t} d\mathbf{x} + \frac{1}{2} \left(\Psi_{i_{\mathcal{E}}}^{K,\text{Rus}}(\mathbf{u}^{(0)}, \varepsilon^{(0)}) + \Psi_{i_{\mathcal{E}}}^{K,\text{Rus}}(\mathbf{u}^{(k)}, \varepsilon^{(k)}) \right). \quad (30)$$

Finally, the high-order limited residuals are computed similarly to (15) as

$$\Phi_{i_{\mathcal{V}},ts}^{K,L} = \beta_{i_{\mathcal{V}}}^K \Phi_{ts}^K, \quad \Psi_{i_{\mathcal{E}},ts}^{K,L} = \beta_{i_{\mathcal{E}}}^K \Psi_{ts}^K, \quad (31)$$

where the space-time Rusanov residuals (29) and (30) are used in expressions analogous to (16) to calculate $\beta_{i_{\mathcal{V}}}^K$ and $\beta_{i_{\mathcal{E}}}^K$, respectively:

$$\beta_{i_{\mathcal{V}}}^K = \frac{\max\left(\frac{\Phi_{i_{\mathcal{V}},ts}^{K,\text{Rus}}}{\Phi_{ts}^K}, 0\right)}{\sum_{j_{\mathcal{V}} \in K} \max\left(\frac{\Phi_{j_{\mathcal{V}},ts}^{K,\text{Rus}}}{\Phi_{ts}^K}, 0\right)}, \quad (32)$$

and

$$\beta_{i_{\mathcal{E}}}^K = \frac{\max\left(\frac{\Psi_{i_{\mathcal{E}},ts}^{K,\text{Rus}}}{\Psi_{ts}^K}, 0\right)}{\sum_{j_{\mathcal{E}} \in K} \max\left(\frac{\Psi_{j_{\mathcal{E}},ts}^{K,\text{Rus}}}{\Psi_{ts}^K}, 0\right)}, \quad (33)$$

and

$$\begin{aligned} \Phi_{ts}^K &= \sum_{i_{\mathcal{V}} \in K} \Phi_{i_{\mathcal{V}},ts}^{K,\text{Rus}} = \int_K \left(\rho \frac{\widetilde{\delta^k \mathbf{u}}}{\Delta t} + \frac{1}{2} \left(\nabla_{\mathbf{x}} p^{(0)} + \nabla_{\mathbf{x}} p^{(k)} \right) \right) d\mathbf{x}, \\ \Psi_{ts}^K &= \sum_{i_{\mathcal{E}} \in K} \Psi_{i_{\mathcal{E}},ts}^{K,\text{Rus}} = \int_K \left(\rho \frac{\widetilde{\delta^k \varepsilon}}{\Delta t} + \frac{1}{2} \left(p^{(0)} \nabla_{\mathbf{x}} \cdot \mathbf{u}^{(0)} + p^{(k)} \nabla_{\mathbf{x}} \cdot \mathbf{u}^{(k)} \right) \right) d\mathbf{x}. \end{aligned}$$

Next, we introduce

$$C_{i_V}^{\mathcal{V},K} = \int_K \rho \varphi_{i_V} d\mathbf{x}, \quad C_{i_\varepsilon}^{\mathcal{E},K} = \int_K \rho \psi_{i_\varepsilon} d\mathbf{x}.$$

After applying the mass lumping as in (19), (20), the mass matrices \mathbf{M}_V for the velocity and \mathbf{M}_ε for the thermodynamics become diagonal with entries at the diagonals given by

$$\begin{aligned} C_{i_V}^{\mathcal{V}} &= \int_\Omega \rho \varphi_{i_V} d\mathbf{x} = \sum_{K \ni i_V} \int_K \rho \varphi_{i_V} d\mathbf{x}, \\ C_{i_\varepsilon}^{\mathcal{E}} &= \int_\Omega \rho \psi_{i_\varepsilon} d\mathbf{x} = \sum_{K \ni i_\varepsilon} \int_K \rho \psi_{i_\varepsilon} d\mathbf{x}. \end{aligned}$$

Both matrices are invertible because $\varphi_{i_V} > 0$ and $\psi_{i_\varepsilon} > 0$ in the element since we are using Bézier basis. Note that we could have omitted the mass lumping for the thermodynamic relation because the mass matrix is block diagonal.

By construction, the scheme is conservative for the velocity, however, nothing is guaranteed for the specific energy. In order to solve this issue, inspired by the calculations of section 3, and given a set of velocity residuals $\{\Phi_{i_V}^K\}$ and internal energy residuals $\{\Psi_{i_\varepsilon}^K\}$, we slightly modify the internal energy evaluation by defining

$$(34) \quad \Psi_{i_\varepsilon,ts}^{K,c} = \Psi_{i_\varepsilon,ts}^{K,L} + r_{i_\varepsilon},$$

where the correction term r_{i_ε} is chosen to ensure the discrete conservation properties and will be specified in the following section.

With all the above definitions, the resulting residual distribution scheme is written as follows: for $k = 0, 1$

$$(35a) \quad C_{i_V}^{\mathcal{V}} \frac{\mathbf{u}_{i_V}^{(k+1)} - \mathbf{u}_{i_V}^{(k)}}{\Delta t} + \sum_{K \ni i_V} \Phi_{i_V,ts}^{K,L} = 0,$$

$$(35b) \quad C_{i_\varepsilon}^{\mathcal{E}} \frac{\varepsilon_{i_\varepsilon}^{(k+1)} - \varepsilon_{i_\varepsilon}^{(k)}}{\Delta t} + \sum_{K \ni i_\varepsilon} \Psi_{i_\varepsilon,ts}^{K,c} = 0,$$

$$(35c) \quad \frac{\mathbf{x}_{i_V}^{(k+1)} - \mathbf{x}_{i_V}^n}{\Delta t} = \frac{1}{2} \left(\mathbf{u}_{i_V}^n + \mathbf{u}_{i_V}^{(k)} \right).$$

Note that the discretization (35c) is nothing but a second-order SSP RK scheme.

6. Conservation and entropy production. Here we first derive the expression for the term r_{i_ε} to ensure the local conservation property of the residual distribution scheme (35) and then give some conditions on the discrete entropy production.

6.1. Discrete conservation. The continuous problem satisfies the following conservation property for the specific total energy $e = \frac{1}{2} \mathbf{u}^2 + \varepsilon$:

$$(36) \quad \int_K \rho \frac{de}{dt} dx + \int_{\partial K} p \mathbf{u} \cdot \mathbf{n} d\sigma = 0.$$

The numerical scheme has to satisfy a conservation property analogous to (36) at the discrete level. To achieve this, the thermodynamic residual has been modified according to (34).

The term r_{i_ε} is chosen such that:

$$(37) \quad \sum_{i_\nu \in K} \mathbf{u}_{i_\nu} \left(C_{i_\nu}^{\mathcal{V},K} \left(\frac{\delta^k \mathbf{u}_{i_\nu}}{\Delta t} - \widetilde{\frac{\delta^k \mathbf{u}_{i_\nu}}{\Delta t}} \right) + \Phi_{i_\nu}^{K,L} \right) + \sum_{i_\varepsilon \in K} \left(C_{i_\varepsilon}^{\mathcal{E},K} \left(\frac{\delta^k \varepsilon_{i_\varepsilon}}{\Delta t} - \widetilde{\frac{\delta^k \varepsilon_{i_\varepsilon}}{\Delta t}} \right) + \Psi_{i_\varepsilon,ts}^{K,L} + r_{i_\varepsilon} \right) = 0.$$

Since we have only one constraint, we impose in addition that $r_{i_\varepsilon} = r$ for any i_ε , so that from (37) we can derive

$$(38) \quad r_{i_\varepsilon} = \frac{1}{N_K^K} \left(\int_{\partial K} \hat{p}_n \mathbf{u} d\sigma - \sum_{i_\nu \in K} \mathbf{u}_{i_\nu} \Phi_{i_\nu}^{K,L} + \sum_{i_\nu \in K} C_{i_\nu}^{\mathcal{V},K} \frac{\delta^k \mathbf{u}_{i_\nu}}{\Delta t} - \sum_{i_\varepsilon \in K} \Psi_{i_\varepsilon}^{K,L} + \sum_{i_\varepsilon \in K} C_{i_\varepsilon}^{\mathcal{E},K} \frac{\delta^k \varepsilon_{i_\varepsilon}}{\Delta t} \right),$$

where \hat{p}_n is the approximation of the pressure flux $p\mathbf{n}$ at the boundary of the element K .

So far, we have indicated a way to recover local conservation by adding a term to the internal energy equation. This term depends on the residuals that are themselves constructed from first order residuals and in turn depend on the pressure flux, so that the conservation property is valid for any pressure flux. It is possible to add further constraints for better conservation properties and in this section we show how to impose a local (semi-discrete) entropy inequality. We also state two results that are behind the construction.

6.2. Entropy balance. Since at the continuous level

$$T \frac{ds}{dt} = \frac{d\varepsilon}{dt} + p \frac{dv}{dt},$$

where $v = 1/\rho$ is the specific volume, and knowing that

$$\rho \frac{dv}{dt} = \nabla_{\mathbf{x}} \cdot \mathbf{u},$$

we look at the entropy inequality

$$(39) \quad \int_K \rho T \frac{ds}{dt} = \int_K \rho \left(\frac{d\varepsilon}{dt} + p \frac{dv}{dt} \right) d\mathbf{x} = \int_K \left(\rho \frac{d\varepsilon}{dt} + p \nabla_{\mathbf{x}} \cdot \mathbf{u} \right) d\mathbf{x} \geq 0$$

and try to derive its discrete counterpart.

For the sake of simplicity we demonstrate the discrete entropy balance conditions on the first-order version of the scheme (35). Taking the sum over the degrees of freedom of an element K in equation (35b) and noting that in the first-order scheme

496 $\widetilde{\delta^k \varepsilon} / \Delta t = 0$ and $\Psi_{i_\varepsilon}^{K,L} = \Psi_{i_\varepsilon}^{K,\text{Rus}}$, we get

497

$$\begin{aligned}
 498 \quad (40) \quad & \sum_{i_\varepsilon \in K} C_{i_\varepsilon}^{\mathcal{E},K} \frac{\delta^k \varepsilon_{i_\varepsilon}}{\Delta t} + \sum_{i_\varepsilon \in K} \Psi_{i_\varepsilon}^{K,c} \\
 499 \quad & = \sum_{i_\varepsilon \in K} \left(\int_K \rho \psi_{i_\varepsilon} d\mathbf{x} \right) \frac{\delta^k \varepsilon_{i_\varepsilon}}{\Delta t} + \sum_{i_\varepsilon \in K} (\Psi_{i_\varepsilon}^{K,\text{Rus}} + r_{i_\varepsilon}) = \int_K \rho \frac{\delta^k \varepsilon}{\Delta t} d\mathbf{x} + \Psi^K + \sum_{i_\varepsilon \in K} r_{i_\varepsilon} \\
 500 \quad & = \int_K \left(\rho \frac{\delta^k \varepsilon}{\Delta t} + p \nabla_{\mathbf{x}} \cdot \mathbf{u} \right) d\mathbf{x} + \sum_{i_\varepsilon \in K} r_{i_\varepsilon} = 0.
 \end{aligned}$$

501

502 The first term in (40) is a discrete analogue of (39), therefore we can require

$$503 \quad \int_K \left(\rho \frac{\delta^k \varepsilon}{\Delta t} + p \nabla_{\mathbf{x}} \cdot \mathbf{u} \right) d\mathbf{x} \geq 0,$$

504 which yields another constraint on r_{i_ε} :

$$505 \quad (41) \quad \sum_{i_\varepsilon \in K} r_{i_\varepsilon} \leq 0.$$

506 We note that the derivation of the entropy condition for a general high-order scheme
 507 is slightly more tedious, however, it leads to exactly the same condition (41) and is
 508 therefore not presented here.

509 Let us show that the entropy condition (41) holds for the first order residual
 510 distribution scheme. From the conservation condition (38) we have

$$511 \quad r_{i_\varepsilon} = \frac{1}{N_{\mathcal{E}}^K} \left(\int_{\partial K} \hat{p}_n \mathbf{u} d\sigma - \sum_{i_\nu \in K} \mathbf{u}_{i_\nu} \Phi_{i_\nu}^{K,\text{Rus}} - \sum_{i_\varepsilon \in K} \Psi_{i_\varepsilon}^{K,\text{Rus}} \right),$$

512 and therefore

513

$$\begin{aligned}
 514 \quad (42) \quad & \sum_{i_\varepsilon \in K} r_{i_\varepsilon} = \int_{\partial K} \hat{p}_n \mathbf{u} d\sigma - \sum_{i_\nu \in K} \mathbf{u}_{i_\nu} \Phi_{i_\nu}^{K,\text{Rus}} - \sum_{i_\varepsilon \in K} \Psi_{i_\varepsilon}^{K,\text{Rus}} \\
 515 \quad & = \int_{\partial K} \hat{p}_n \mathbf{u} d\sigma - \sum_{i_\nu \in K} \mathbf{u}_{i_\nu} \Phi_{i_\nu}^K - \alpha_K \sum_{i_\nu \in K} \mathbf{u}_{i_\nu} (\mathbf{u}_{i_\nu} - \bar{\mathbf{u}}) - \sum_{i_\varepsilon \in K} \Psi_{i_\varepsilon}^K - \alpha_K \sum_{i_\varepsilon \in K} (\varepsilon_{i_\varepsilon} - \bar{\varepsilon}) \\
 516 \quad & = \int_{\partial K} \hat{p}_n \mathbf{u} d\sigma - \int_K \mathbf{u} \cdot \nabla_{\mathbf{x}} p d\mathbf{x} - \alpha_K \sum_{i_\nu \in K} (\mathbf{u}_{i_\nu} - \bar{\mathbf{u}})^2 - \int_K p \nabla_{\mathbf{x}} \cdot \mathbf{u} d\mathbf{x} \\
 517 \quad & = -\alpha_K \sum_{i_\nu \in K} (\mathbf{u}_{i_\nu} - \bar{\mathbf{u}})^2 \leq 0,
 \end{aligned}$$

518

519 where we have taken into account that

$$520 \quad \sum_{i_\nu \in K} \mathbf{u}_{i_\nu} (\mathbf{u}_{i_\nu} - \bar{\mathbf{u}}) = \sum_{i_\nu \in K} (\mathbf{u}_{i_\nu} - \bar{\mathbf{u}})^2, \quad \text{and} \quad \sum_{i_\varepsilon \in K} (\varepsilon_{i_\varepsilon} - \bar{\varepsilon}) = 0.$$

521 Therefore, the entropy condition (41) is satisfied with any $\alpha_K \geq 0$.

522 For high order schemes it doesn't seem to be possible to recast the entropy con-
 523 dition (41) explicitly in terms of α_K as it is done in (42) for the first order scheme
 524 since α_K is only implicitly used to calculate the limiting coefficients $\beta_{i_\nu}^K$ and $\beta_{i_\varepsilon}^K$, by

(32), (33). Therefore, in practice, in order to ensure the entropy inequality in the high order scheme we add an edge stabilization term to the velocity residual:

$$(43) \quad \Phi_{i_V}^{K,stab} = \sum_{e \in \partial K} h^2 \theta \int_e [\nabla_{\mathbf{x}} \cdot \mathbf{u}] [\nabla_{\mathbf{x}} \varphi_{i_V}] \cdot \mathbf{n} d\sigma,$$

where $\theta > 0$ is a coefficient that can be estimated and $[f] = f^+ - f^-$ is the jump of f at the interface, see [12] for more details.

6.3. Results on conservation and entropy inequality. Using the same technique as in [5], we can easily state the following two results:

PROPOSITION 6.1 (Conservation). *Assume that we are given a set of regular meshes which characteristic size h tends to zero. Consider the time $t > 0$ so that the meshes mapped by the transformation (1) stay regular. Assume that the scheme (35), with the residuals defined as in section 5 generate solutions that are bounded in L^∞ by a constant that only depends on the family of meshes and the initial conditions. If a sub-sequence of these solutions converges towards \mathbf{u} , ε , then this is a weak solution of the Euler equations.*

A weak solution satisfies an entropy inequality under certain conditions which are specified by the following result.

PROPOSITION 6.2 (Entropy). *If in addition to the assumptions of Proposition 6.1 the energy correction satisfies (41), then the limit solution satisfies*

$$\rho T \frac{ds}{dt} \geq 0$$

in the sense of distributions.

7. Second order scheme in one-dimensional case. In this section, we specify in detail the algorithm of the second order residual distribution scheme in the one-dimensional case. Hereafter, X and x denote the Lagrangian and Eulerian coordinates, respectively, and the scalar velocity is denoted by u .

Lets start by giving the one dimensional version of (9). We have

$$(44) \quad \begin{aligned} u(x, t) &= \frac{dx}{dt}, x = \Phi(X, t) \\ J(x, t) \rho(x, t) &= \rho(X, 0) := \rho_0(X), \\ \rho \frac{du}{dt} + \frac{\partial p}{\partial x} &= 0 \\ \rho \frac{d\varepsilon}{dt} + p \frac{\partial u}{\partial x} &= 0. \end{aligned}$$

We assume that $X \in [a, b] = \Omega_0$ and introduce a moving grid with nodes x_i , $i = 0, \dots, N$ and set $K := [x_j, x_{j+1}]$. The kinematic space \mathcal{V} is formed by the continuous quadratic Bézier elements in Ω_0 while the thermodynamic space \mathcal{E} has a piecewise-linear basis. As before, we denote by $\mathcal{D}_{\mathcal{V}}$ (resp. $\mathcal{D}_{\mathcal{E}}$) the set of degrees of freedom in \mathcal{V} (resp. \mathcal{E}).

The algorithm of the one-dimensional second order scheme for integrating (44) consists of two steps.

559 **Step 1:** calculate $u^{(1)}, \varepsilon_h^{(1)}, x_h^{(1)}$. For any $i_v \in \mathcal{D}_v$ and $i_\varepsilon \in \mathcal{D}_\varepsilon$

$$\begin{aligned}
 & C_{i_v}^v \frac{u_{i_v}^{(1)} - u_{i_v}^n}{\Delta t} + \sum_{K \ni i_v} \beta_{i_v}^K \int_K \frac{\partial p_h^n}{\partial x} dx = 0, \\
 & C_{i_\varepsilon}^\varepsilon \frac{\varepsilon_{i_\varepsilon}^{(1)} - \varepsilon_{i_\varepsilon}^n}{\Delta t} + \sum_{K \ni i_\varepsilon} \left[\beta_{i_\varepsilon}^K \int_K p_h^n \frac{\partial u^n}{\partial x} dx + r_{i_\varepsilon}^{(0)} \right] = 0, \\
 & \frac{x_{i_v}^{(1)} - x_{i_v}^n}{\Delta t} = u_{i_v}^n,
 \end{aligned}$$

561 where $\beta_{i_v}^K$ (resp. $\beta_{i_\varepsilon}^K$) is evaluated using (32) (resp. (33)) with $k = 0$, and the
 562 correction term $r_{i_\varepsilon}^{(0)}$ is defined via (38).

563 **Step 2:** calculate $u^{n+1}, \varepsilon_h^{n+1}, x_h^{n+1}$. For any $i_v \in \mathcal{D}_v$ and $i_\varepsilon \in \mathcal{D}_\varepsilon$,

$$\begin{aligned}
 & C_{i_v}^v \frac{u_{i_v}^{n+1} - u_{i_v}^{(1)}}{\Delta t} + \sum_{K \ni i_v} \beta_{i_v}^K \int_K \left(\rho_h^n \frac{u^{(1)} - u^n}{\Delta t} + \frac{1}{2} \left(\frac{\partial p_h^n}{\partial x} + \frac{\partial p_h^{(1)}}{\partial x} \right) \right) dx = 0, \\
 & C_{i_\varepsilon}^\varepsilon \frac{\varepsilon_{i_\varepsilon}^{n+1} - \varepsilon_{i_\varepsilon}^{(1)}}{\Delta t} + \sum_{K \ni i_\varepsilon} \left[\beta_{i_\varepsilon}^K \int_K \left(\rho_h^n \frac{\varepsilon_h^{(1)} - \varepsilon_h^n}{\Delta t} + \frac{1}{2} \left(p_h^n \frac{\partial u^n}{\partial x} + p_h^{(1)} \frac{\partial u^{(1)}}{\partial x} \right) \right) dx + r_{i_\varepsilon}^{(1)} \right] = 0, \\
 & \frac{x_{i_v}^{n+1} - x_{i_v}^{(1)}}{\Delta t} = \frac{1}{2} (u_{i_v}^n + u_{i_v}^{(1)}),
 \end{aligned}$$

565 where again $\beta_{i_v}^K$ (resp. $\beta_{i_\varepsilon}^K$) is defined using (32), (resp. (33)) for $k = 1$, and the
 566 correction term $r_{i_\varepsilon}^{(1)}$ is calculated via (38).

567 The density $\rho(x, t)$, when needed, is evaluated via the local relation $\rho(x, t) =$
 568 $J(x, t)\rho_0(X)$, where J is the Jacobian of the coordinate transformation, i.e. determi-
 569 nant of the matrix defined by (2) and ρ_0 is the density in the initial configuration.
 570 Note that the mesh is legal as long as J stays strictly positive.

571 **8. Numerical results.** To assess the accuracy and robustness of the proposed
 572 residual distribution scheme we solve a series of shock tube problems. For numerical
 573 experiments of this section we shall use the following EOS:

- 574 • ideal EOS: $p = (\gamma - 1)\rho\varepsilon$, where $\gamma > 1$,
- 575 • stiffened EOS: $p = (\gamma - 1)\rho\varepsilon - \gamma p_s$,
- 576 • Jones-Wilkins-Lee (JWL) EOS: $p = (\gamma - 1)\rho\varepsilon + f_j(\rho)$, where

$$f_j(\rho) = A_1 \left(1 - \frac{(\gamma - 1)\rho}{R_1 \bar{\rho}} \right) \exp \left(- \frac{R_1 \bar{\rho}}{\rho} \right) + A_2 \left(1 - \frac{(\gamma - 1)\rho}{R_1 \bar{\rho}} \right) \exp \left(- \frac{R_1 \bar{\rho}}{\rho} \right).$$

578 If not explicitly specified, the gas is supposed to be modeled by the ideal EOS with
 579 $\gamma = 1.4$.

580 We use the technique proposed in [20] to control the time step and in all numerical
 581 tests the CFL number is set to 0.5.

582 **8.1. Numerical convergence study.** We test the accuracy of our scheme on a
 583 smooth isentropic flow problem similar to the test case introduced in [15]. The initial
 584 data for our test problem is the following:

$$\rho_0(x) = 1 + 0.9999995 \sin(2\pi x), \quad u_0(x) = 0, \quad p_0(x) = \rho^\gamma(x, 0), \quad x \in [-1, 1].$$

with polytropic index $\gamma = 3$ and periodic boundary conditions.

The exact density and velocity in this case can be obtained by the method of characteristics and is explicitly given by

$$\rho(x, t) = \frac{1}{2}(\rho_0(x_1) + \rho_0(x_2)), \quad u(x, t) = \sqrt{3}(\rho(x, t) - \rho_0(x_1)),$$

where for each coordinate x and time t the values x_1 and x_2 are solutions of the nonlinear equations

$$x + \sqrt{3}\rho_0(x_1)t - x_1 = 0,$$

$$x - \sqrt{3}\rho_0(x_2)t - x_2 = 0.$$

Fig. 2 shows the errors of the flow parameters in the L_1 -norm with respect to the number of DOFs at time $T = 0.08$ for three different residual distribution schemes using Bezier basis: first-order RD scheme with modified time stepping and mass lumping (denoted by "B1/B0"), second-order RD scheme with modified time stepping and mass lumping ("B2/B1") and the second-order RD scheme with classical second-order Runge-Kutta time stepping ("B2/B1 RK2"). It can be clearly seen that the first-order "B1/B0" and second-order "B2/B1" schemes reach the expected convergence rates for the velocity and a little bit more than first order for the thermodynamical variables. The order of the formally second-order "B2/B1 RK2" scheme drops to first, which is the result of the loss of accuracy due to mass lumping applied in a standard time stepping algorithm.

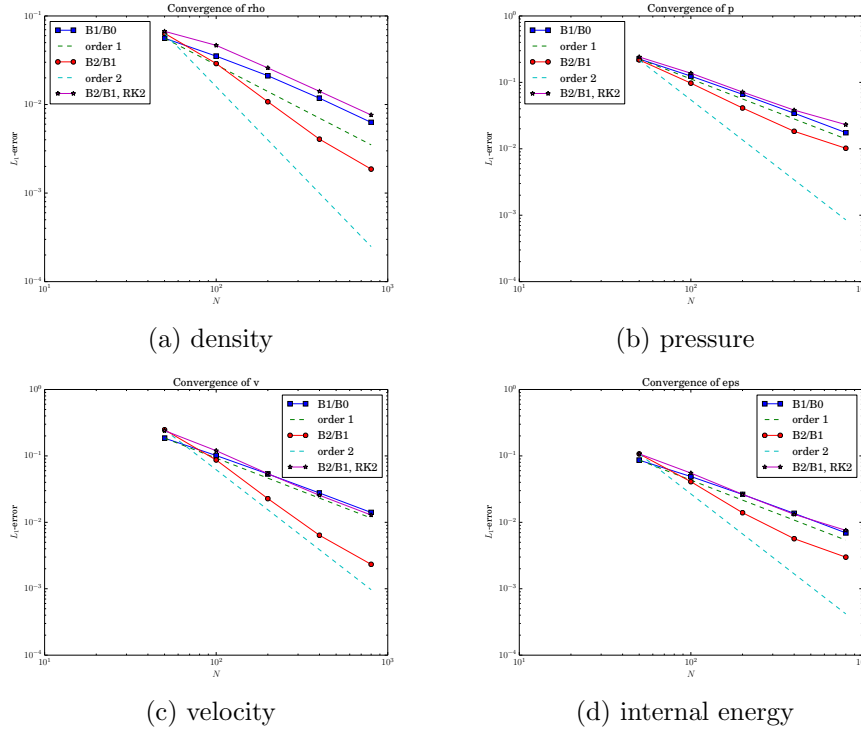


FIG. 2. Convergence history for the smooth isentropic test problem

8.2. The Sod shock tube. The Sod's shock tube is a classical test problem for the assessment of the numerical methods for solving the Euler equations. Its solution consists of a left rarefaction, a contact and a right shock wave. The initial data for this problem is given as follows:

$$(\rho_0, u_0, p_0) = \begin{cases} (1.0, 0.0, 1.0), & x < 0, \\ (0.125, 0.0, 0.1), & x > 0. \end{cases}$$

The results for first-order ("B1/B0") and second-order ("B2/B1") schemes are shown in Fig. 3. Obviously, the second-order scheme provides better resolution of the smooth flow regions such as the left rarefaction wave, while both schemes give an accurate approximation of the contact discontinuity and the right shock wave. On Fig.

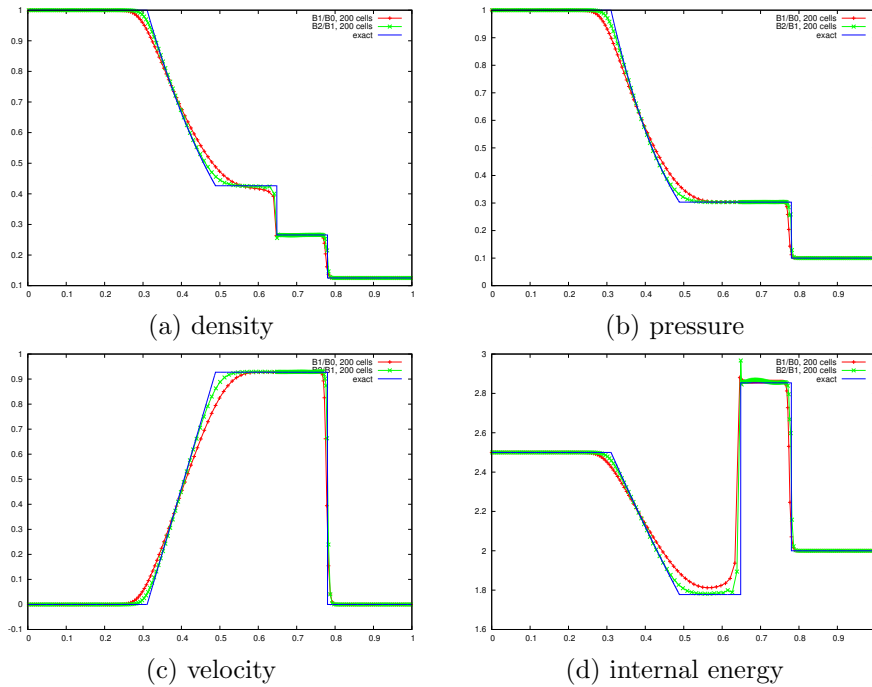


FIG. 3. Solution of the Sod shock tube problem at $T = 0.16$

3-(d), the reader can see that the internal energy exhibits an overshoot at the contact, this one is connected to the small undershoot of the density on Fig. 3-(a), while the velocity and the pressure behave as expected over the contact. This phenomena is typical of Lagrangian schemes, one can consult for example [26] for similar results with first and higher order schemes, or [24] for a series of benchmark tests such as Sod's and the blast wave case we consider in section 8.5 where a similar behaviour exist. The reason is that there is no diffusion mechanism across interface, since mesh points move exactly at the speed of the contact. In Eulerian methods, or ALE ones, where the mesh point do not move or move at velocities that are not the fluid ones, this drawback do not exist. But some diffusion exist accros the contact lines: all depends on the physics that one wish to capture accurately.

8.3. 123-problem. The 123-problem [30] is a classical benchmark case to test the behavior of the numerical method for low-density and low-pressure flows. The

628 initial data is the following:

$$629 \quad (\rho_0, u_0, p_0) = \begin{cases} (1.0, -2.0, 0.4), & -4 \leq x < 0, \\ (1.0, 2.0, 0.4), & 0 < x \leq 4. \end{cases}$$

630 The solution of this problem consists of two rarefaction waves traveling in opposite
631 directions, so that a low-density and low-pressure region is generated in between.

632 The numerical solution illustrated in Fig. 4 shows that the low intermediate density
633 and pressure are captured correctly by both first-order and second-order RD
634 scheme, the latter being more accurate for the internal energy. The insufficient res-
635 olution of the flow near the vacuum is a well-known phenomenon for Lagrangian
636 schemes, and is related to the strong heating phenomenon, see e.g. [15, 32, 33].

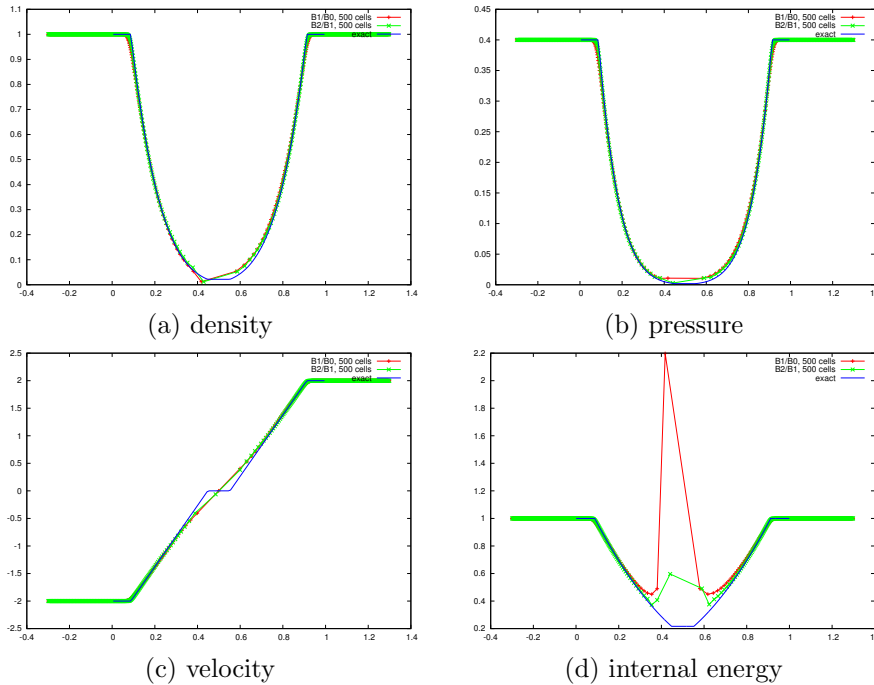
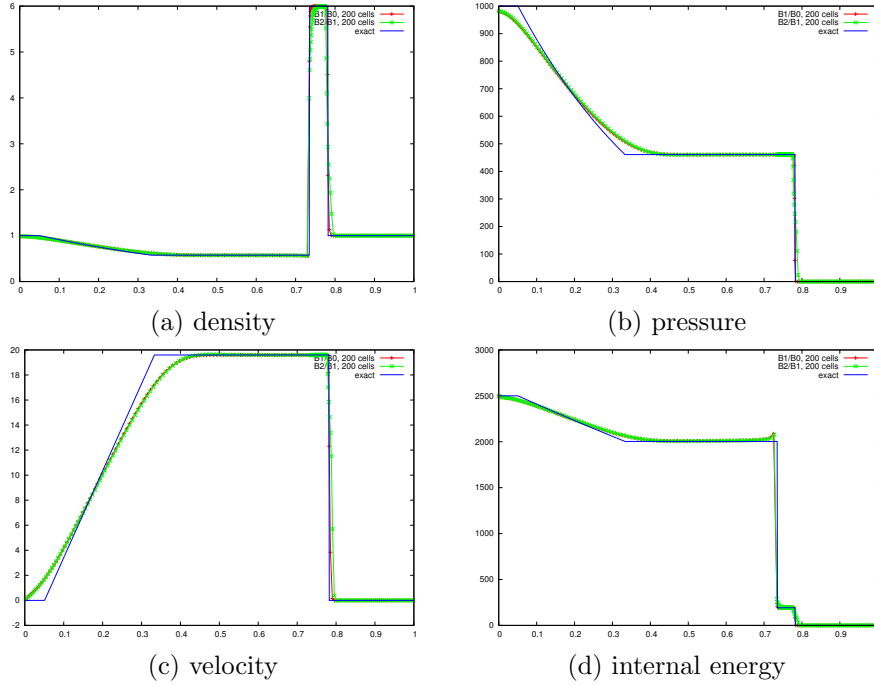


FIG. 4. Solution of the 123-problem at $T = 0.15$

637 **8.4. Strong shock.** This test case is actually the left half of the blast wave
638 problem of Woodward and Colella [36]. It's a severe test problem containing a left
639 rarefaction wave, a contact discontinuity and a strong right shock wave and it is often
640 used to assess the robustness of the numerical methods for fluid dynamics [30]. The
641 initial data for this test problem is

$$642 \quad (\rho_0, u_0, p_0) = \begin{cases} (1.0, 0.0, 1000.0), & x < 0, \\ (1.0, 0.0, 0.01), & x > 0. \end{cases}$$

643 The simulation results shown in Fig. 5 indicate that both first and second-order
644 schemes are robust and can accurately resolve strong shocks.

FIG. 5. Solution of the strong shock problem at $T = 0.012$

8.5. Interaction of blast waves. The interaction of blast waves is a standard low energy benchmark problem involving strong shocks reflecting from the walls of the tube with further mutual interaction. The initial data is the following:

$$\rho_0 = 1, \quad u_0 = 1, \quad p_0 = \begin{cases} 10^3, & 0 \leq x < 0.1, \\ 10^{-2}, & 0.1 < x < 0.9, \\ 10^2, & 0.9 < x \leq 1. \end{cases}$$

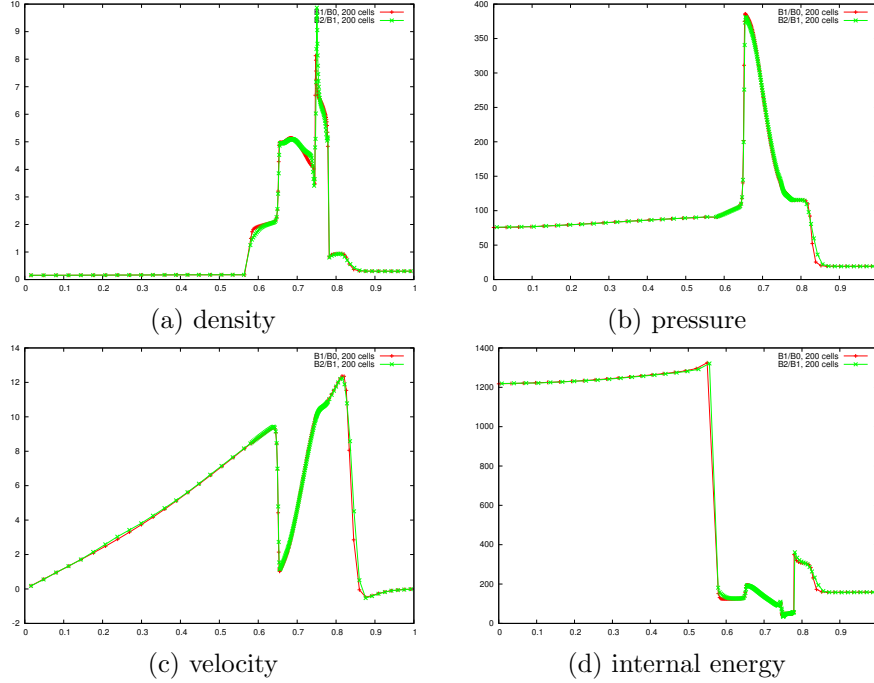
Reflective boundary conditions are applied at $x = 0$ and $x = 1$.

The results are displayed on Fig. 6. We can make the same comments as above, namely that the contacts are very well represented with a slight overshoot of the thermodynamical variables across the contact.

8.6. Gas-liquid shock tube. This severe water-air shock tube problem is used to assess the performance of the numerical schemes for multi-material flows with a strong interfacial contact discontinuity. In this problem, the fluid to the left-hand side of the membrane initially located at $x = 0.3$ is a perfect gas with $\gamma = 1.4$ in the ideal EOS, while the fluid to the right of the membrane is water modeled by the stiffened EOS with $\gamma = 4.4$ and $p_s = 6 \cdot 10^8$. The initial parameters of the two fluids are the following:

$$(\rho_0, u_0, p_0) = \begin{cases} (5.0, 0.0, 10^5), & 0 \leq x < 0.3, \\ (10^3, 0.0, 10^9), & 0.3 < x \leq 1. \end{cases}$$

The computational results for the first and second-order RD schemes shown in Fig. 7 demonstrate a very good agreement with the exact solution and, what is im-

FIG. 6. Solution of the Woodward-Colella blast wave interaction problem at $T = 0.038$

portant, a very accurate resolution of the interfacial contact discontinuity by both schemes.

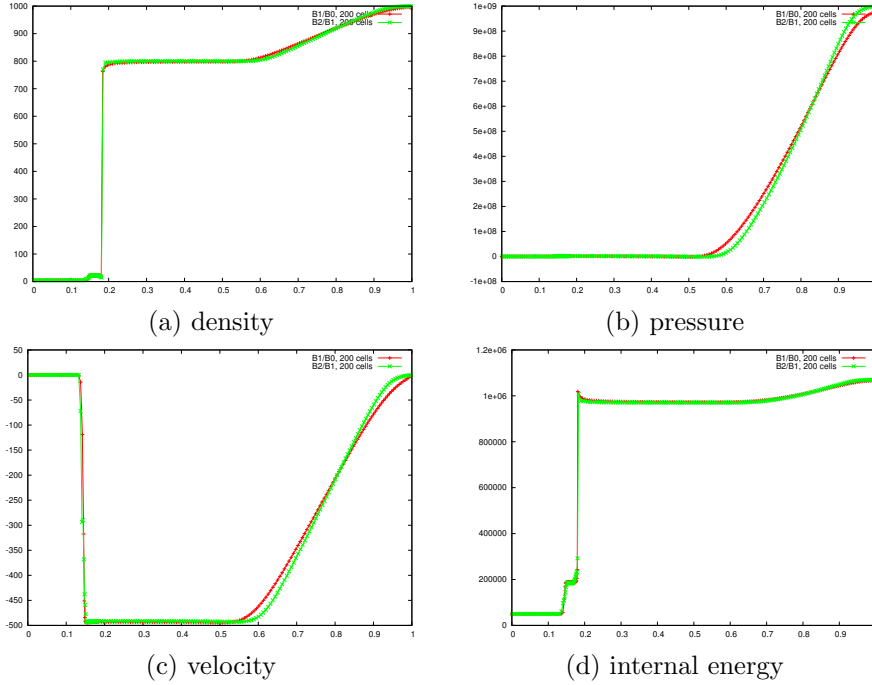
8.7. Underwater TNT explosion. This 1D spherically symmetric underwater detonation problem [19] is often used as a benchmark to test the robustness of the methods for multi-phase problems with general equation of state. The initial condition consists of the detonation products phase on the left of the initial discontinuity and the water phase to the right. We consider the stiffened version of the classical TNT explosion problem proposed in [15], which is more likely to produce negative density and/or internal energy.

To the left of the interface initially located at $x = 0.16$, the gaseous product of the detonated explosive is modeled by the JWL EOS with $A_1 = 3.712 \cdot 10^5$, $A_2 = 3.23 \cdot 10^3$, $R_1 = 4.15$, $R_2 = 0.95$, $\bar{\rho} = 1.63 \cdot 10^{-3}$ and $\gamma = 1.3$. On the right of the interface, the water is described through the stiffened EOS with $\gamma = 7.15$ and $p_s = 3.309 \cdot 10^2$. Initial data for this test problem is:

$$(\rho_0, u_0, p_0) = \begin{cases} (1.63 \cdot 10^{-3}, 0.0, 8.381 \cdot 10^3), & 0 \leq x < 0.16, \\ (1.025 \cdot 10^{-3}, 0.0, 1.0), & 0.16 < x \leq 3. \end{cases}$$

The results are shown in Fig.8. Clearly, both first and second-order RD schemes capture the interfaces very accurately, while second-order scheme is more accurate in the regions of smooth flow.

8.8. Comparison with the Eulerian version of the scheme. The Eulerian version of the scheme uses a collocated mesh and the one dimensional variant of the scheme described in [27] with mass lumping. We compare on a soft case (Sod, Fig. 9)

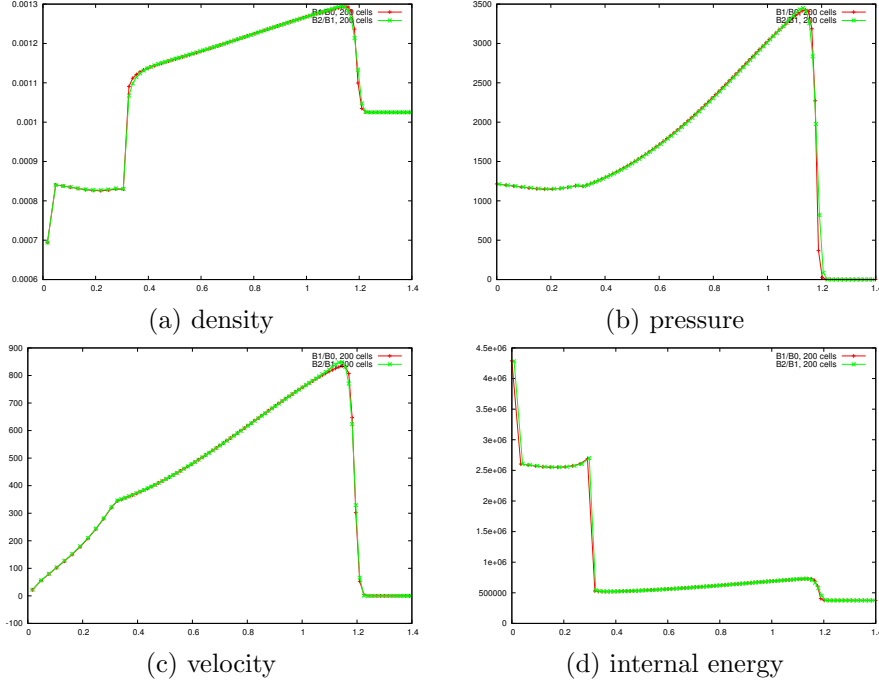
FIG. 7. Solution of the gas-liquid shock tube problem at $T = 0.00024$

and a more difficult one (Collela and Woodward, Fig. 10). The results are in good agreement: the shock travel at the same speed. We can notice that the density is more accurate across the contact discontinuity for the Lagrangian simulation as expected. There are two shocks, one for $x \approx 0.7$ and one for $x \approx 0.9$. The first one seems sharper for the Lagrangian scheme, the second one by the Eulerian one. In the two cases, it is not a surprise since the mesh density becomes higher at the shock for the Lagrangian simulations. The contact are also crisper for the Lagrangian simulation, We also see that the fan seems better represented for these versions of the schemes, without clear reason.

9. Conclusions. In this paper we have proposed a Residual Distribution (RD) scheme for the Lagrangian hydrodynamics based on the staggered finite element formulation of [16]. We have developed an efficient mass matrix diagonalization algorithm which relies on the modification of the time-stepping scheme and gives rise to an explicit high order accurate scheme. Moreover, the scheme is parameter-free and doesn't require any artificial viscosity. The one-dimensional numerical tests considered in this paper show the robustness of the method for problems involving very strong shock waves. A comparison between the Lagrangian and Eulerian formulations confirms that contact discontinuities are very well described.

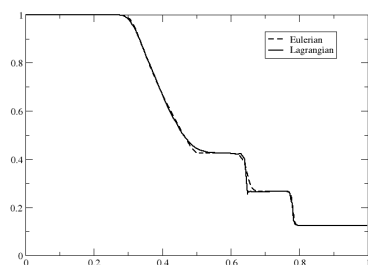
One of the contributions of this paper is to show how one can discretise a *non conservative* version of the Euler equation and guarantee that the correct weak solutions are recovered. This problem has already be considered by other authors such as [23, 22], but we believe our strategy is simpler and can work for any order of accuracy. It has been further illustrated on multifluid and multiphase problems, see [2].

Further research includes the extension of the present method to multiple dimen-

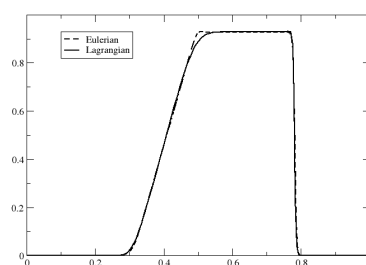
FIG. 8. *Solution of the underwater TNT explosion problem at $T = 0.00025$*

708 sions and higher order in space and time.

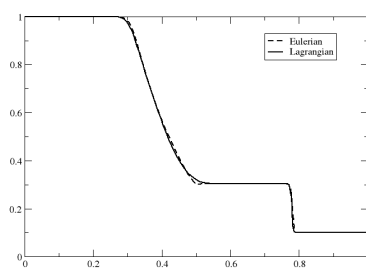
709 **Acknowledgments.** We thank Dr. A. Barlow from AWE, UK, for introducing
 710 us to this problem. We have had several very interesting conversations on this topic,
 711 and the selection of numerical examples has also been influenced by these discus-
 712 sion. The authors thanks the financial support of the Swiss SNF via the grant #
 713 200021_153604 ("High fidelity simulation for compressible material"). R.A. has been
 714 partially supported by this grant and S.T. has been fully supported by this grant.



(a) Density

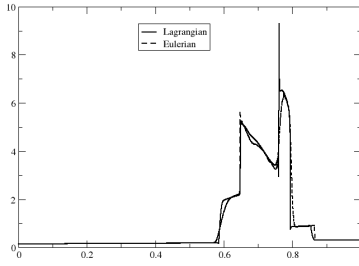


(b) Velocity

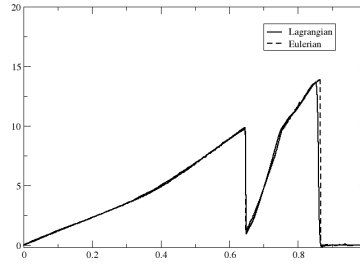


(c) Pressure

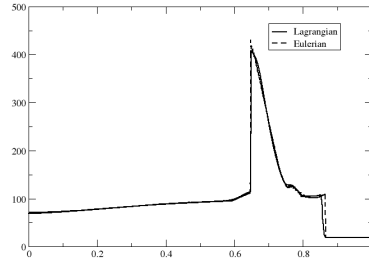
FIG. 9. Comparison of the present scheme (B2/B1) and its second order Eulerian version for the Sod case. The meshes have 200 cells, the $CFL=0.25$ for the Lagrangian scheme and 0.5 for the Eulerian one.



(a) Density



(b) Velocity



(c) Pressure

FIG. 10. Comparison of the present scheme (B2/B1) and its second order Eulerian version for the Colella case. The meshes have 1000 cells, the CFL=0.25 for the Lagrangian scheme and 0.5 for the Eulerian one.

REFERENCES

- [1] R. ABGRALL, *On a class of high order schemes for hyperbolic problems*, in Proceedings of the International Congress of Mathematicians, S. Y. Jang, Y. R. Kim, D.-W. Lee, and I. Yie, eds., vol. IV, 2014, pp. 699–726. ISBN 978-89-6105-807-0.
- [2] R. ABGRALL, P. BACIGALUPPI, AND S. TOKAREVA, *A high-order nonconservative approach for hyperbolic equations in fluid dynamics*. <https://hal.archives-ouvertes.fr/hal-hal-01327473v1>.
- [3] R. ABGRALL, P. BACIGALUPPI, AND S. TOKAREVA, *How to avoid mass matrix for linear hyperbolic problems*, in Proceeding of ENUMATH 2015, vol. Lecture Notes in Computational Science and Engineering, Springer, 2016.
- [4] R. ABGRALL, A. LARAT, AND M. RICCHIUTO, *Construction of very high order residual distribution schemes for steady inviscid flow problems on hybrid unstructured meshes*, J. Comput. Phys., 230 (2011).
- [5] R. ABGRALL AND P. ROE, *High order fluctuation schemes on triangular meshes*, J. Sci. Comput., 19 (2003), pp. 3–36.
- [6] A. BARLOW, *A compatible finite element multi-material ALE hydrodynamics algorithm*, Internat. J. Numer. Methods Fluids, 56 (2007), pp. 953–964.
- [7] W. BOSCHERI, D. BALSARA, AND M. DUMBSER, *Lagrangian ADER-WENO finite volume schemes on unstructured triangular meshes based on genuinely multidimensional HLL Riemann solvers*, J. Comput. Phys., 267 (2014), pp. 112–138.
- [8] W. BOSCHERI AND M. DUMBSER, *Arbitrary-Lagrangian-Eulerian one-step WENO finite volume schemes on unstructured triangular meshes*, Comm. Comp. Phys., 14 (2013), pp. 1174–1206.
- [9] W. BOSCHERI AND M. DUMBSER, *A direct Arbitrary-Lagrangian-Eulerian ADER-WENO finite volume scheme on unstructured tetrahedral meshes for conservative and non-conservative hyperbolic systems in 3D*, J. Comput. Phys., 275 (2014), pp. 484–523.
- [10] W. BOSCHERI, M. DUMBSER, AND O. ZANOTTI, *High order cell-centered Lagrangian-type finite volume schemes with time-accurate local time stepping on unstructured triangular meshes*, J. Comput. Phys., 291 (2015), pp. 120–150.
- [11] W. BOSCHERI, R. LOUBÈRE, AND M. DUMBSER, *Direct Arbitrary-Lagrangian-Eulerian ADER-MOOD finite volume schemes for multidimensional hyperbolic conservation laws*, J. Comput. Phys., 292 (2015), pp. 56–87.
- [12] E. BURMAN AND P. HANSBO, *Edge stabilization for Galerkin approximation of convection-diffusion-reaction problems*, Comput. Methods Appl. Mech. Engrg., 193 (2004), pp. 1437–1453.
- [13] E. J. CATAMANA, D. E. BURTON, AND M. J. SHASHKOV, *The construction of compatible hydrodynamics algorithms utilizing conservation of total energy*, J. Comput. Phys., 146 (1998), pp. 227–262.
- [14] J. CHENG AND C.-W. SHU, *A high order eno conservative Lagrangian type scheme for the compressible Euler equations*, J. Comput. Phys., 227 (2007), pp. 1567–1596.
- [15] J. CHENG AND C.-W. SHU, *Positivity-preserving Lagrangian scheme for multi-material compressible flow*, J. Comput. Phys., 257 (2014), pp. 143–168.
- [16] V. DOBREV, T. KOLEV, AND R. RIEBEN, *High order curvilinear finite element methods for Lagrangian hydrodynamics*, SIAM J. Sci. Comput., 34 (2012), pp. B606–B641.
- [17] M. DUMBSER, *Arbitrary-Lagrangian-Eulerian ADER-WENO finite volume schemes with time-accurate local time stepping for hyperbolic conservation laws*, Comp. Meth. Appl. Mech. Eng., 280 (2014), pp. 57–83.
- [18] M. DUMBSER AND W. BOSCHERI, *High-order unstructured Lagrangian one-step WENO finite volume schemes for non-conservative hyperbolic systems: Applications to compressible multi-phase flows*, Computers & Fluids, 86 (2013), pp. 405–432.
- [19] C. FARHAT, J.-F. GERBEAU, AND A. RALLU, *Fiver: a finite volume method based on exact two-phase Riemann problems and sparse grids for multi-material flows with large density jumps*, J. Comput. Phys., 231 (2012), pp. 6360–6379.
- [20] G. GEORGES, J. BREIL, AND P.-H. MAIRE, *A 3D GCL compatible cell-centered Lagrangian scheme for solving gas dynamics equations*, J. Comput. Phys., 305 (2016), pp. 921–941.
- [21] M. E. GURTIN, E. FRIED, AND L. ANAND, *The Mechanics and Thermodynamics of Continua*, Cambridge University Press, 2010.
- [22] R. HERBIN, W. KHERIJ, AND J.-C. LATCHÉ, *On some implicit and semi-implicit staggered schemes for the shallow water and Euler equations*, ESAIM, Math. Model. Numer. Anal., 48 (2014), pp. 1807–1857, <http://dx.doi.org/10.1051/m2an/2014021>.
- [23] R. HERBIN, J.-C. LATCHÉ, AND T. NGUYEN, *Explicit staggered schemes for the compressible*

- 776 *Euler equations.*, ESAIM, Proc., 40 (2013), pp. 83–102, [http://dx.doi.org/10.1051/proc/](http://dx.doi.org/10.1051/proc/201340006)
 777 [201340006](http://dx.doi.org/10.1051/proc/201340006).
- 778 [24] R. LOUBERE, *Validation test case suite for compressible hydrodynamics computation.* [http:](http://loubere.free.fr/images/test_suite.PDF)
 779 [//loubere.free.fr/images/test_suite.PDF](http://loubere.free.fr/images/test_suite.PDF).
- 780 [25] P.-H. MAIRE, R. ABGRALL, J. BRIL, AND J. OVADIA, *A cell-centered Lagrangian scheme for*
 781 *two-dimensionnal compressible flow problems*, SIAM J. Sci. Comput., 29 (2007), pp. 1781–
 782 1824.
- 783 [26] C. MUNZ, *On Godunov type schemes for Lagrangian gas dynamics*, SIAM J. Numer. Anal., 31
 784 (1994), pp. 17–42.
- 785 [27] M. RICCHIUTO AND R. ABGRALL, *Explicit runge-kutta residual-distribution schemes for time*
 786 *dependent problems*, J. Comput. Phys., 229 (2010), pp. 5653–5691.
- 787 [28] G. SCOVAZZI, , M. CHRISTON, T. HUGHES, AND J. SHADID, *Stabilized shock hydrodynamics: I*
 788 *A Lagrangian method*, Comput. Methods Appl. Mech., 196 (2007), pp. 923–966.
- 789 [29] M. SHASKHOV, P. MAIRE, RIEBEN, AND A. BARLOW, *Review of Lagrangian methods*, J. Comput.
 790 Phys., (2016).
- 791 [30] E. F. TORO, *Riemann Solvers and Numerical Methods for Fluid Dynamics*, Springer-Verlag,
 792 2009.
- 793 [31] F. VILAR, P.-H. MAIRE, AND R. ABGRALL, *A discontinuous galerkin discretization for solving*
 794 *the two-dimensional gas dynamics equations written under total Lagrangian formulation*
 795 *on general unstructured grids*, J. Comput. Phys., 276 (2014), pp. 188–234.
- 796 [32] F. VILAR, C. SHU, AND P.-H. MAIRE, *Positivity-preserving cell-centered Lagrangian schemes*
 797 *for multi-material compressible flows: From first-order to high-orders. part i: The one-*
 798 *dimensional case*, J. Comput. Phys., 312 (2016), pp. 385–415.
- 799 [33] F. VILAR, C. SHU, AND P.-H. MAIRE, *Positivity-preserving cell-centered Lagrangian schemes*
 800 *for multi-material compressible flows: From first-order to high-orders., part ii: The two-*
 801 *dimensional case*, J. Comput. Phys., 312 (2016), pp. 416–442.
- 802 [34] J. VON NEUMANN AND R. D. RICHTMYER, *A method for the numerical calculation of hydrody-*
 803 *namics shocks*, J. Appl. Phys., 21 (1950), pp. 232–237.
- 804 [35] M. L. WILKINS, *Methods in Computational Physics*, vol. 3, Academic Press, New York, 1964.
- 805 [36] P. WOODWARD AND P. COLELLA, *The numerical simulation of two-dimensional fluid flow with*
 806 *strong shocks*, J. Comput. Phys., 54 (1984), pp. 115–173.